ACS OMEGA

http://pubs.acs.org/journal/acsodf

Review

Asphaltenes: Aggregates in Terms of A1 and A2 or Island and Archipielago Structures

Socrates Acevedo* and Jimmy Castillo

Cite This: *ACS Omega* 2023, 8, 4453−4471

Read Online

ACCESS | Metrics & More | Article Recommendations

ABSTRACT: In this work several issues related to asphaltenes and asphaltene aggregates such as isolation of real asphaltene molecules and comparison of these with average structures obtained using regular analytics laboratory techniques are presented. Several molecular organic models were used to simulate asphaltene in solution and aggregates formation in the two solvents toluene and THF employed. The results, obtained from simulation calculations using molecular dynamics were compared with experimental chromatography results obtained using the micro gel permeation chromatography (μGPC), inductively coupled plasma (ICP) mass spectra (MS) combined technique (GPC ICP MS for short). In this case reasonable hydrodynamic ratios and size distribution were obtained for asphaltenes and their corresponding subfractions A1 and subfraction A2. Comparison between experimental sample profiles, transmission of electron microscopy (TEM) data, and molecular dynamics allows for estimation of hydrodynamic ratios of around 8 nm. Highly aromatic and island type molecular model A30 and continental type molecular model A40 were employed in the molecular dynamics to built colloids. In this case open-like colloids (A40) and compact-like colloids A30 were obtained. Subjects such as trapped compounds (TC), metallic porphyrins, and colloidal dipole moments were also studied. Studies of the adsorption behavior of asphaltenes on several macroscopic and nanoscopic surfaces are presented and show the tendency of the asphaltene to adsorb in aggregate form.

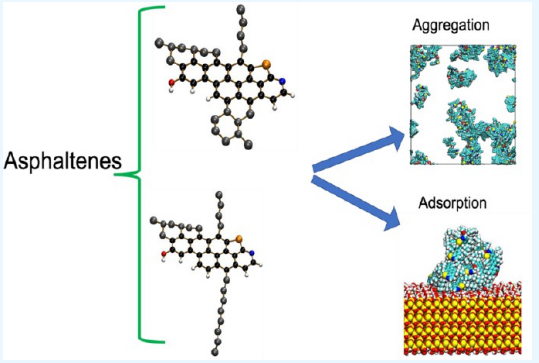

INTRODUCTION

The present work is mainly devoted to the study of asphaltene structure in THF solution both from the experimental and theoretical point of view. As it is well-known the words island and archipelago have been use to vaguely suggest a structure with one core, as is the case for island-type, and several cores to designate an archipelago-like structure. To our knowledge, and setting aside the A1 and A2 asphaltene subfractions, there is no experimental information consistent with the above archipelago- and core-type structures. As it is described below, we collect GPC results and other experimental data which are consistent with flexible chains for A2 subfrations and consequently with large hydrodynamic ratios which emerge at very short retention times. These finding were discovered after studing several asphaltene samples, and thus we could conclude that both island- and archipelago-type structures are present in asphaltene mixtures with different compositions. The average structure of these subfractions has a decisive importance in the interaction of the sufractions and the subsequent aggregation and adsorption on surfaces, These phenomena are widely known and studied using very general approximations that usually do not take into consideration the impact that the island or archipelago structures may have on these processes. In the present work a review and analysis of this impact on the shape of the aggregates and their interaction with surfaces is made. The density of these structures and their capacity to trap crude constituent compounds is another phenomenon of great interest in the industry, due to the economic implications. The present review provides information and analysis on the importance of the these trapped compounds in the asphaltene aggregate, especially the vanadium and niquel pophyrins-like molecules.

REAL AND HYPOTHETICAL STRUCTURE OF ASPHALTENES

Asphaltenes, by definition, are the "fraction of crude oil soluble in toluene and insoluble in heptane". This is an operational definition which paradoxically fits well for this highly complex mixture. A good description of this material can be found in the literature.[1]

Perhaps, the asphaltene definition would benefit from some of its average characteristics such as low average H/C value (close to 1.15), aromaticity close to 50%, and nitrogen with averages

Received: October 2, 2022
Accepted: January 4, 2023
Published: January 23, 2023

https://doi.org/10.1021/acsomega.2c06362
ACS Omega 2023, 8, 4453−4471

Table 1. Elemental Analysis of Asphaltene Samples from Venezuela[a]

Asphaltene	1	2	3	4	5	6	Mean Values
C	84.28	83.67	83.67	83.42	82.43	83.76	83.5
H	7.65	7.45	7.65	7.78	7.66	6.62	7.5
N	1.56	1.67	1.42	1.66	1.65	1.68	1.6
O	1.2	1.19	1.37	1.11	1.35	1.37	1.3
S	4.01	4.63	4.26	4.5	5.07	5.07	4.6
	98.7	98.61	98.37	98.47	98.16	98.5	98.5
H/C	1.089	1.068	1.097	1.119	1.115	0.948	1.07
N/C	0.016	0.017	0.015	0.017	0.017	0.017	0.07
O/C	0.011	0.011	0.012	0.010	0.012	0.012	0.01
S/C	0.127	0.148	0.136	0.144	0.164	0.161	0.15

[a]The similar atomic values reveal similar type of oil (extra heavy oil).

Table 2. Averages Molecular Weight Formula

C	H	N	O	S
42	46	0.67	0.6	0.75

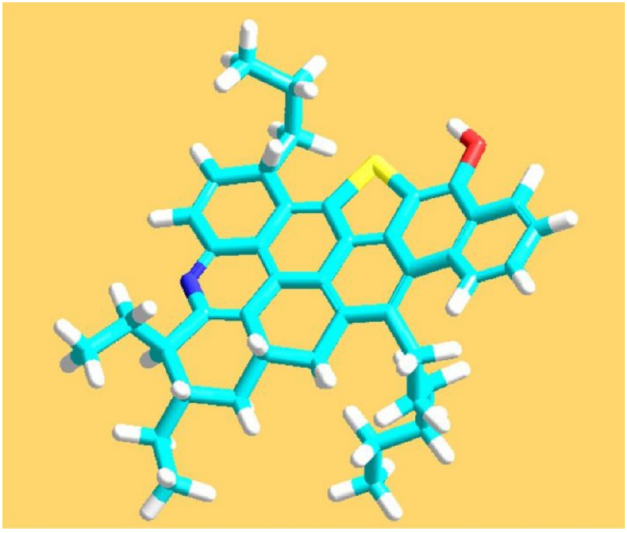

Figure 1. Hypothetical molecular model or structure coherent with the above molecular formula and coherent with the experimental data described above. (AHS: asphaltene hypothetical structure)

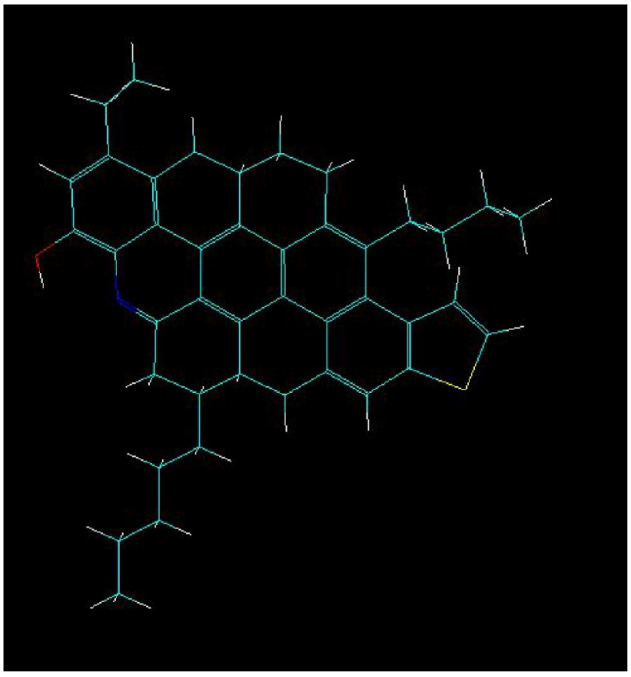

Figure 2. Another view of the hypothetical structure depicted in Figure 1.

between 1 and 2%, usually with relatively high sulfur content. In Table 1 some elemental analysis of samples from Venezuela are shown.

Oxygen was measured directly affording lower than expected values. As calculated recently oxygen content was a primer source of sample aggregation (see below). H/C average values in this table are a bit lower (1.07) than the one mentioned above (1.15). This may be a consequence of samples in Table 1 being obtained from extra heavy oil and consequently with a relatively higher quantity of carbon.

Using values in Table 1 and an average molecular mass of 600 g/mol,[2] the average molecular formula could be obtained as seen in Table 2.

It is worth noting that the above formula is based on experimental results corresponding to this particular mixture, and any other similar formula corresponding to another asphaltene mixture would be different. Fractionated atomic indices are expected in any compound mixture, and asphaltenes are not an exception.

Using the ^{13}C nuclear magnetic resonance technique. it is possible to obtain spectra from which the number of aromatic and aliphatic carbons in the molecule could be obtained. In the present case these values are both close to 50%. Combining the above information, the structure shown below could be proposed as coherent with the experimental data gathered.

Figures 1 and 2 collect the usual asphaltene sectors: functional groups of the average structure such an aromatic core, dangling aliphatic chains, pyridine type amine, phenol type OH, and tiophene type sulfur.

Using a similar strategy other average or hypothetical structures have been proposed in the past.[2−10] Catalogs of many structures have been reported.[3] Use of these hypothetical structures in structural aspects is now common place among those interested in molecular and aggregation issues.

■ ATOMIC FORCE MICROSCOPY (AFM)

Using AFM methods, the isolation and the characterization of asphaltene molecules have been achieved.[11] We refer to these asphaltenes as AFMAs. In Table 3 we collected atomic and molecular indexes which could be compared with experimental values corresponding to bulk-asphaltenes which we nominate as

https://doi.org/10.1021/acsomega.2c06362
ACS Omega 2023, 8, 4453−4471

Table 3. Description of Elemental Analysis and Other Indices of Asphaltenes Reported in the Literature (ARL)

Sample	Title	C	H	H/C	MM	N	O	S	ALC	%	DBE
1	A1 0	49	32	0.653	680.87	2	0	1	5	89.80	35
2	A1. 3	52	33	0.635	719.9	1	0	0	6	88.46	37
3	A1.4	40	22	0.550	582.74	0	0	0	3	92.50	30
4	A1.9	39	29	0.744	511.6	1	0	0	8	79.49	26
5	A1.6b	93	104	1.118	1109.64	0	0	0	33	64.52	42
6	A1.14	49	32	0.653	652.85	0	0	1	7	85.71	34
7	A1.16	36	22	0.611	454.57	0	0	0	2	94.44	26
8	A1.22	29	20	0.690	400.54	0	0	1	3	89.66	20
9	A1.26	71	40	0.563	893.101	0	0	0	5	92.96	52
10	A1.29	34	22	0.647	430.55	0	0	0	6	82.35	24
11	A1.41	40	34	0.850	514.71	0	0	0	8	80.00	24
12	A1.43	44	36	0.818	564.77	0	0	0	11	75.00	27
12	A1.56	58	55	0.948	794.09	3	0	0	16	72.41	33
13	B1.2	53	40	0.755	692,90	0	1	0	7	86.79	34
14	B1.7	52	39	0.750	693.89	1	1	1	7	86.54	34
15	B1.25	52	36	0.692	692.92	0	0	1	4	92.31	35
16	C1 17	32	20	0.625	436.6	0	0	1	2	93.75	23
17	C1 28	39	24	0.615	524.69	0	0	1	3	92.31	28
18	C1.40	45	32	0.711	588.75	0	0	0	8	82.22	30
19	C1.3	28	18	0.643	386.500	0	0	1	2	92.86	20
20	B2.2	61	31	0.508	854	1	1	1	1	98.36	47
21	B2.4	37	29	0.784	487.64	1	0		7	81.08	24
Average		47	34	0.707	617.853					86.069	31

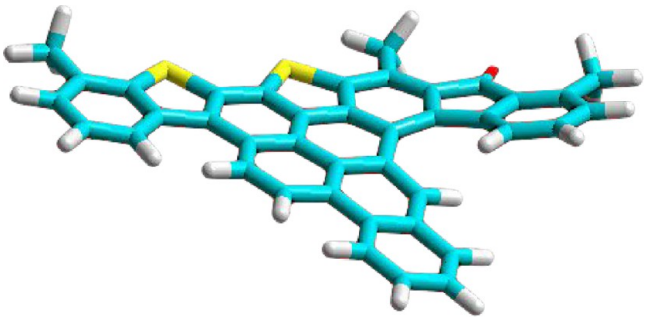

Figure 3. Molecule A1.4. C: 40; H: 22; H/C: 0.55. Low index values (Table2) are probably an artifact of the AFM. Note that the molecule is twisted. Compounds are named using the original names reported.[11] For comparison purposes the naming used in reference 11 has been kept.

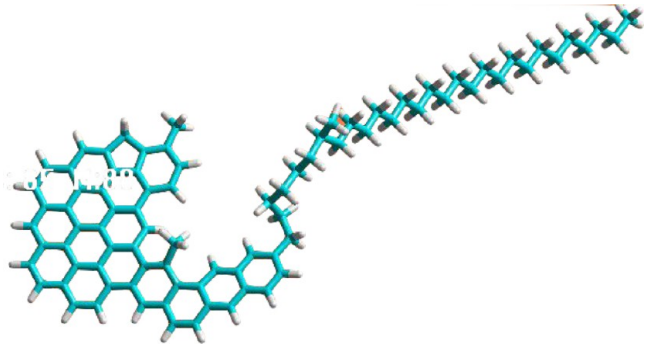

Figure 4. Sample A1.6. C: 85; H:88; MM: 1221.

BAs. Some AFMA structures, taken from reference 11 are depicted in Figures 3 to 5.

Comparison with BAs shows that indexes H/C are too low. On the contrary, aromaticity and DBE are too high for AFMAs. Moreover, the presence of heteroatoms is low, and the absence

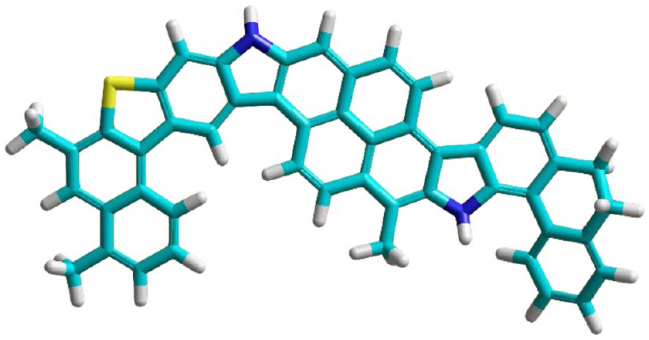

Figure 5. Sample: A1.10. Molecular Formula $C_{52}H_{33}N_2S$. H/C: 0.634; MM: 719.9. Asphaltene structure determined by AFM methods. Compounds are named using the original names reported.[2]

of oxygen is notorious in view of the importance of this atom in the formation of aggregates (see below).

Figure 4 is interesting because being an asphaltene molecule it contains no heteroatoms. Also shows that aliphatic chains could be detected by AFM when the chain is long enough to be adequately adsorbed by the surface.[11] Compounds are named using the original names reported.[11]

In summary in comparison with BAs, AFMAs have too low H/C, too high aromaticity, and too low contents of nitrogen and oxygen. In particular, the presence of phenols should be considered which is coherent with the high capacity of asphaltenes to form aggregates.

AGGREGATION OF ASPHALTENES AND ASPHALTENE MODELS

Hydrogen Bondings. Formation of hydrogen bonding has been mentioned as an important factor in the formation of asphaltene aggregates. Thus, it was observed long ago that in methylation experiments, where phenolic −OH is converted to $-OCH_3$, the number average molecular weight, when measured

https://doi.org/10.1021/acsomega.2c06362
ACS Omega 2023, 8, 4453−4471

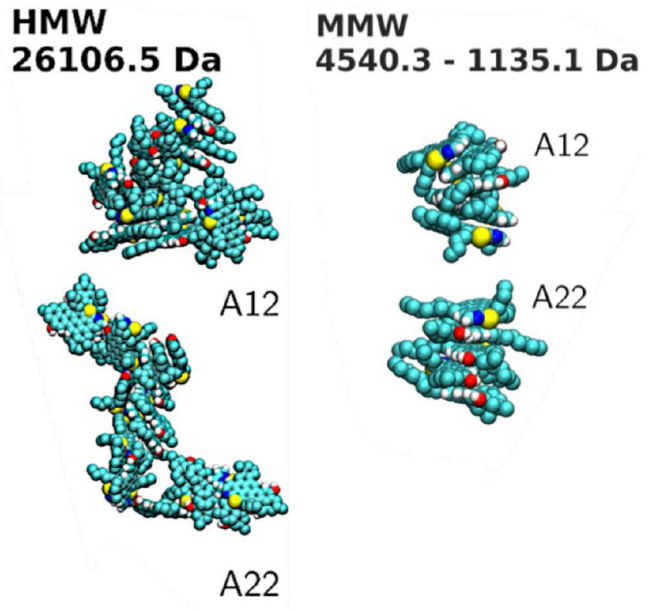

Figure 6. Simulation of aggregation of molecular models in toluene, calculated using molecular dynamics. Note that, in the section on the left, corresponding to the HMW sector, aggregate A22 has the longest hydrodynamics radii (see text).

in toluene at room conditions, dropped from about 10 000 Da to about 2000 Da[12] after methylation of OH functional groups. Moreover, when dissolved in pyridine a vapor pressure osmometry (VPO) was obtained which disclose the importance of hydrogen bonding in asphaltene aggregation. However, methylation and/or polar solvents (pyridine, THF, chloroform, o-dichlorobenzene)[13] afforded VPO values much higher than the now known average close to 700 Da.[2] Possible reasons for such discrepancies are the limitation of VPO to measure at very low concentrations. For instance, to obtain accuracy we should be able to measure at concentrations below 100 mg/kg. However, accurate measurements of asphaltene solutions are possible only above 1 mg/kg.

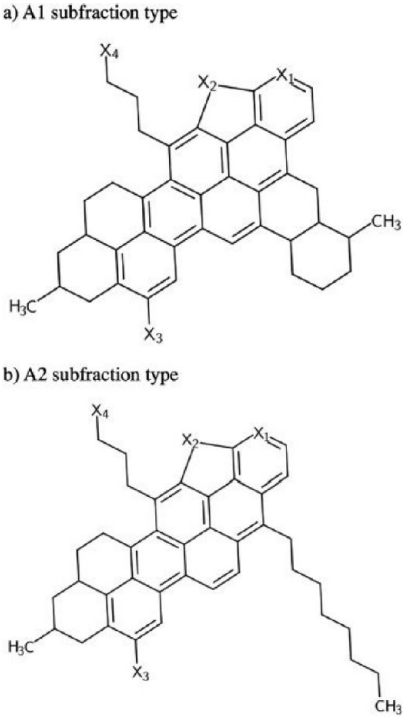

Figure 8. Molecular models used to simulate asphaltene behavior during molecular dynamics within THF or toluene. Note that Model A_{12} contains Model A_1 with S, N, and OH. Similarly model A_{22} is model A_2 with S, N, and OH (aromatic models A30 and A40 are missing).

Molecular Dynamics. To study from a theoretical point of view the forces involved in the aggregation processes of asphaltenes and resins in crude oil, molecular mechanics, and dynamics calculations were carried out for asphaltenes and resins from crude oils of different origins. Average structural models of asphaltenes and their aggregates were used in order to study the forces that determine the association process of asphaltenes and resins in crude oils.[14] Rogel and co-workers found that the contribution of hydrogen bonding energies was comparatively low.

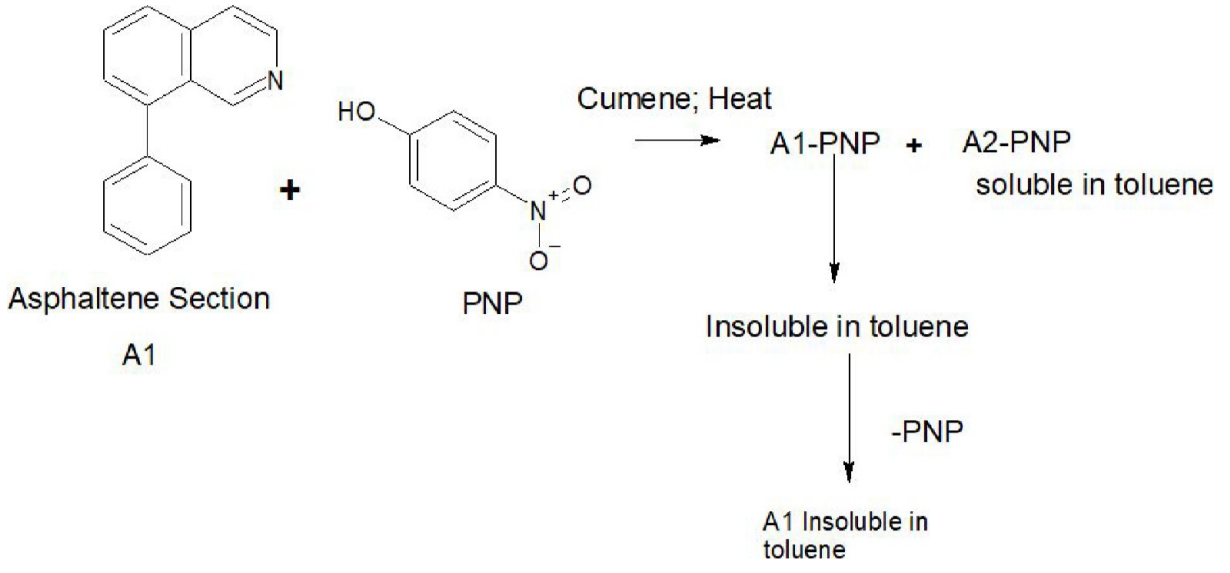

Figure 7. Scheme to illustrate the separation of asphaltenes into subfractions A1, insoluble in toluene, and A2 soluble in toluene.

https://doi.org/10.1021/acsomega.2c06362
ACS Omega 2023, 8, 4453−4471

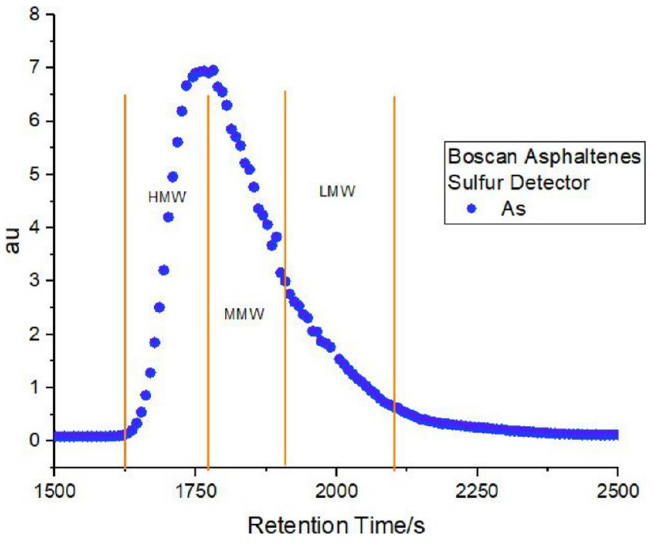

Figure 9. SEC ICP MM chromatographic profile using sulfur detector for asphaltene of Boscan. THF was the mobile phase.

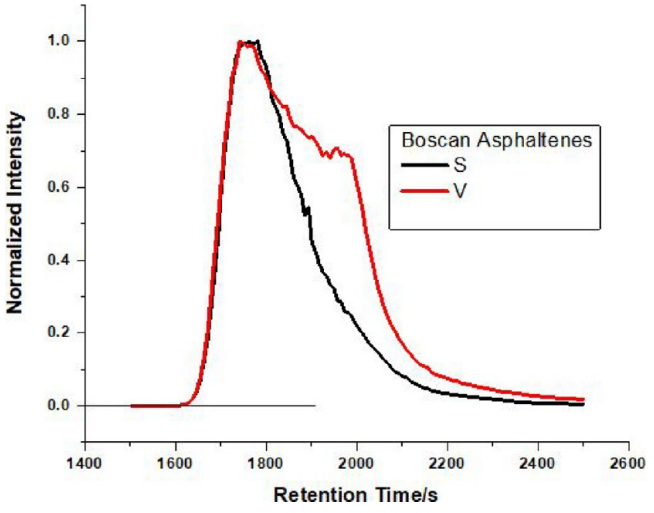

Figure 10. GPC ICP MS profiles using sulfur and vanadium detector corresponding to an asphaltene solution in THF.

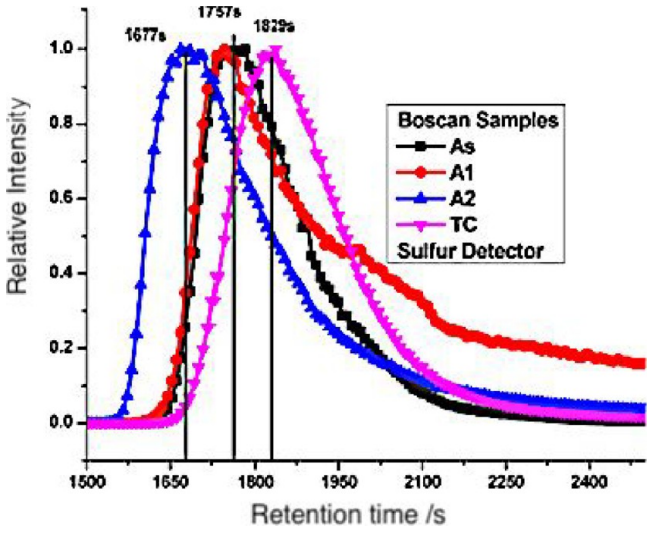

Figure 11. Chromatographic SEC HR ICP MS profiles using sulfur detector corresponding to Boscan samples of asphaltenes (square), subfractions A1 (circle), A2 (triangle up), and trapped compounds (triangle down).

The presence of metallic porphyrins alongside asphaltenes in heavy fractions of crude oil is a key issue in petroleum exploration and upgrading due to its negative impact on the industry.[15] In Santos and co-workers work,[15] molecular dynamics simulations were utilized to investigate complex asphaltene mixtures comprising 10 different molecules; the system was studied under different solvation conditions (toluene/*n*-heptane/water). Authors added nickel and vanadium (under the form of vanadyl) porphyrins with occasionally grafted polar lateral chains, in these mixtures. The authors found that aggregation behavior and interaction with water molecules (as a model to have insights from the interfacial activity of such molecules) are intimately linked to the type of porphyrin and to the molecular properties of the asphaltenes (mainly the presence of polar lateral chains). Vanadium porphyrins, even without polar lateral chains, can form H-bonds that can facilitate the interaction with asphaltenes and might contribute to their presence within asphaltene nanoaggregates. Moreover, when polar lateral chains are present in asphaltene molecules or aggregates, the systems display a supramolecular organization with several distinct interactions at the same time. The shapes of these systems do not totally agree with the traditional average model presented by Yen−Mullins. In the first part of this work, we finally propose that the complex asphaltene structure in complex solvent mixtures seems to have a supramolecular behavior with non-negligent colloidal behavior as well. This should be indicative that Yen−Mullins and Gray's models of asphaltene self-assembly are neither conflictual nor antagonistic, their models show an average behavior of asphaltene solutions. They are two facets of a scale- and molecular structure-dependent complex mechanism. It has been claimed that the presence of water in the mixtures promotes the aggregation of model asphaltenes in solution via hydrogen bonding.[16]

Using density functional theory (DFT), together with organic chemistry molecular models, it has been calculated that hydrogen bonding has a significant contribution to the asphaltene aggregation.[17] It has been suggested that vanadium porphyrins, even without polar lateral chains, can form H-bonds that might contribute to their presence within asphaltene nanoaggregates. According to literature[16] presence of water in the media could increase the stability of aggregates by reinforcing $\pi-\pi$ interactions via water-bridged intermolecular H-bonding between the pyridyl nitrogen and asphaltene aggregate.

Reported by Headen[18] was a classical atomistic molecular dynamics simulation of four structurally diverse molecular model of asphaltenes, a model resin, and their respective mixtures in toluene or heptane under ambient conditions. Relatively large systems (~50 000 atoms) and long time scales (>80 ns) were analyzed. Wherever possible, comparisons are made to available experimental observations asserting the validity of the models. When the asphaltenes are dispersed in toluene, a continuous distribution of cluster sizes is observed with average aggregation number ranging between 3.6 and 5.6, monomers and dimers being the predominant species. As expected for mixtures in heptane, the asphaltene molecules tend to aggregate to form a segregated phase. In these experiments there is no evidence of the multimodal distribution formation of nanoaggregates, and the continuous distribution of clusters is found in character.

https://doi.org/10.1021/acsomega.2c06362
ACS Omega 2023, 8, 4453−4471

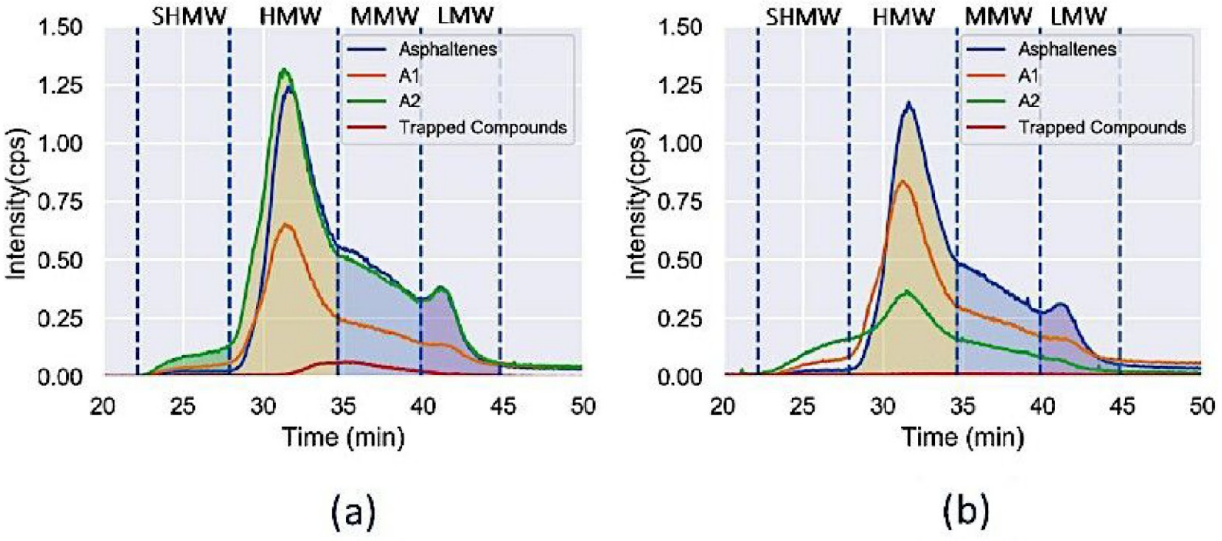

Figure 12. GPC ICP MS chromatography profiles for CN (a) and Hamaca (b) asphaltenes and subfractions A1, A2, and TC, including the super-high-molecular weight (SHMW) zone. Figure reproduced from ref 35. Copyright 2020 American Chemical Society.

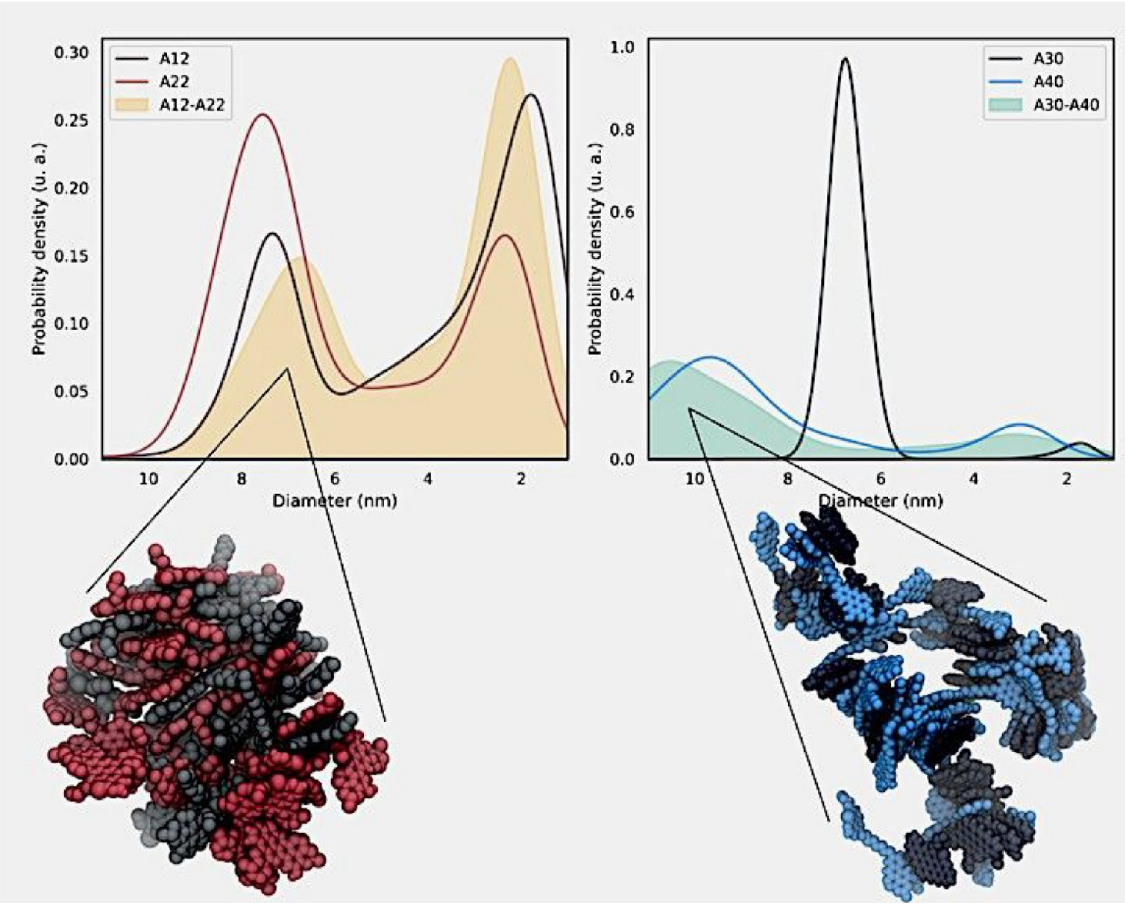

Figure 13. Plot of probability density against the longest hydrodynamic ratios. Arrangement of molecules to form big aggregates; on the left aggregates formed with A12 and A22 molecular models and their 50% mixture; on the right aggregates formed with molecular models A30, A40, and their 50% mixture (see Figure 7). Figure reproduced from ref 67.

Headen reports the aggregation of asphaltenes studied for two asphaltene molecule families, namely, PA3 and CA22 analogues.[18] The chemical characteristics of these proposed molecules were screened by changing the heteroatoms on the backbone and the lateral chain-ends. These molecules were mixed together at different relative concentrations, and for the first time, the aggregation of different asphaltene molecules was determined using molecular dynamics simulations (MDS). The results show that the interaction energies vary depending on the heteroatom arrangement within a given structure and depending

https://doi.org/10.1021/acsomega.2c06362
ACS Omega 2023, 8, 4453−4471

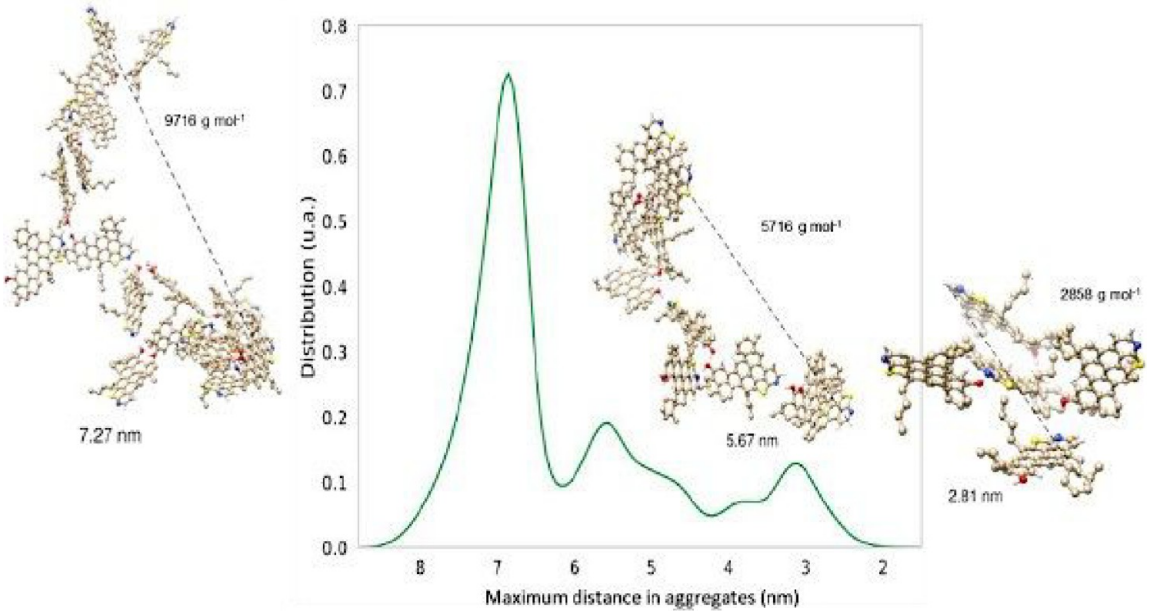

Figure 14. Aggregate distribution curves for A1 models according to their size, displaying three types of aggregates (large, medium, and small). It is qualitatively similar to the experimental GPC-ICP-HR-MS profiles (this work). Figure reproduced from ref 35. Copyright 2020 American Chemical Society.

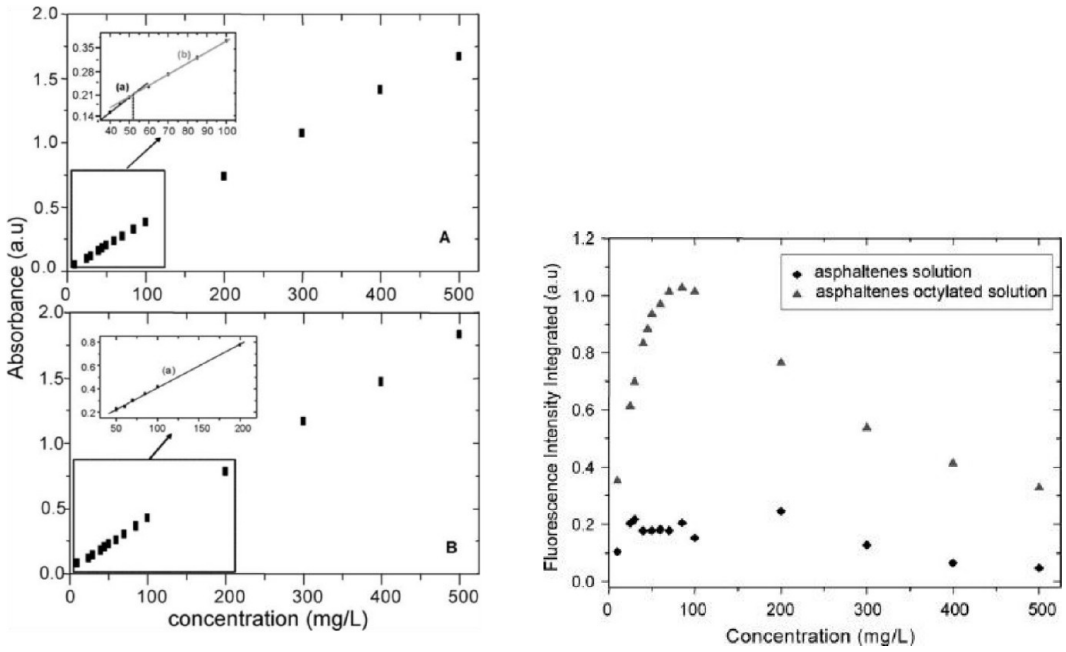

Figure 15. Absorbance (left) figures A and B and fluorescence (right) signal as a function of concentration for solutions of asphaltenes and octylated asphaltenes. Castillo et al.[57] present a paper aimed to study the principal mechanism involved in the adsorption of asphaltene and its subfractions A1 and A2 on to a glass surface using a very sensitive technique as white light interferometry. The experiments were carried out using chloroform as a solvent. This has proven to be is a very good solvent for asphaltene and sub- fractions A1 and A2, even at high concentrations. The use of chloroform allows experiments at high concentrations with a minimum asphaltene aggregation effect. The results presented in this work clearly show first, the importance of the A1 subfraction as responsible for the asphaltene aggregation and subsequent adsorption and, second, the effect of the surface on the density of the molecules near it and consequent increase in the tendency to form aggregates, even using a good solvent. Figure reproduced with permission from ref 56. Copyright 2004 Elsevier.

strongly on the type of asphaltene. Moreover, we showed that the chain-ends have a crucial role in this phenomenon.

The physical chemistry behavior of the heavyweight fraction of crude oil is still a subject of vivid discussions due to the complications which arise in production, transport, and refining from the tendency of this fraction to aggregate.[19] Molecules, that compose the largest part of this fraction, can be separated into two subfractions, A1 and A2, through a treatment with *p*-nitrophenol. In a recent paper published by Acevedo and co-workers,[20] starting from the molecule models suggested by Acevedo, the chemical structure and composition of the two subfractions were modeled and their aggregation mechanism

https://doi.org/10.1021/acsomega.2c06362
ACS Omega 2023, 8, 4453−4471

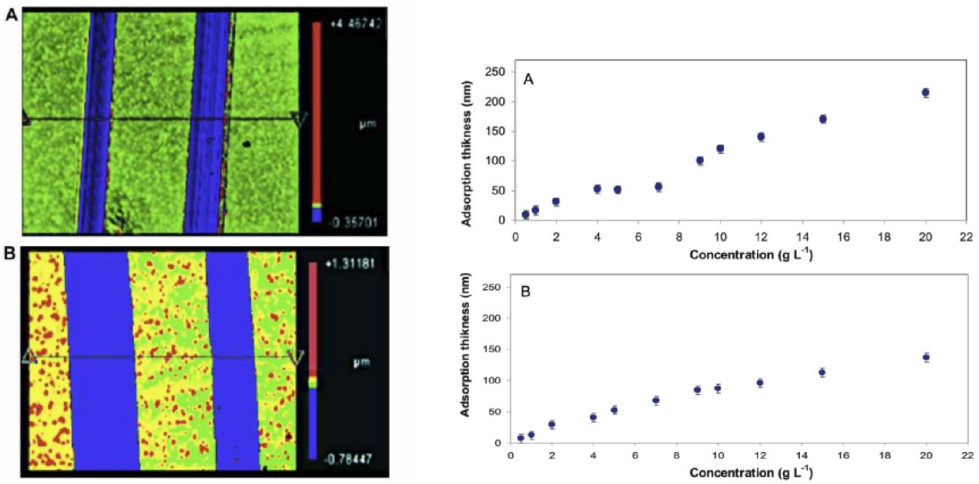

Figure 16. (Left, panels A and B) White light interferometry image of asphaltene subfractions A1 (serie A) and A2 (serie B) adsorbed onto glass surface (blue strips are the clean region). (Right, panels A and B) asphaltene thickness adsorbed as a function of concentration of the solution. Figure reproduced with permission from reference 57. Copyright 2013 Elsevier.

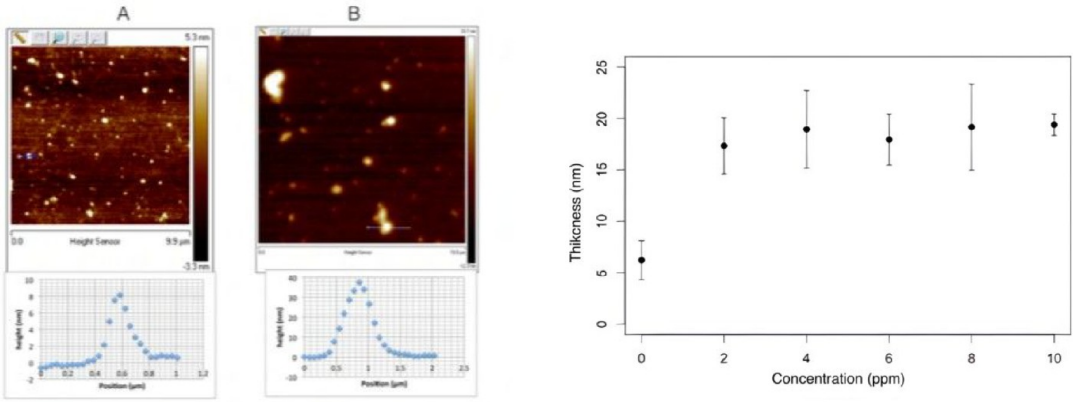

Figure 17. (Left) atomic force microscopy images of nanoparticles before (A) and after (B) asphaltene interaction. (Right) asphaltene recovered thickness as a function of concentration. Figure reproduced with permission from ref 58. Copyright 2017 Elsevier.

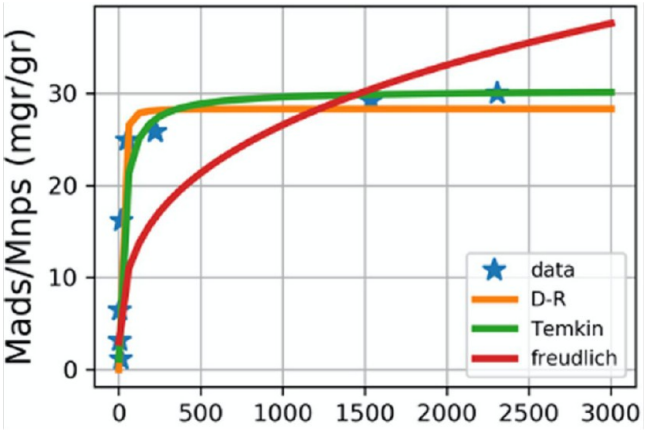

Figure 18. Adsorption plot of asphaltenes onto nanoparticles fitted with different models.

was investigated using classical molecular dynamics simulations. The results in the paper show that oxygen atoms, present as hydroxyl or carboxylic groups, are a key factor in the formation of large aggregate. From the analysis of the simulations, the size of the aggregates was estimated and showed how the different arrangements of the molecules may affect the size of the aggregates. Finally, it was shown that in addition to the structural differences (such as the H/C ratio and DBE) that distinguish the A1 and A2 subfractions, the solubility of the subfractions is also strongly dependent on the ability of the molecules to form hydrogen bonds.

Asphaltene Separation: Subfractions A1 and A2 and Col- Lection of Trapped Compounds. It is now well-known that asphaltene, regardless of its source, could be clearly separated in two subfractions A1 and A2 using the PNP method or *para*-nitrophenol method.[21] In summary a saturated solution of asphaltenes in cumene is boiled and after some time a precipitate of the complex PNP-A1 is formed and the rest (A2-PNP) remains in solution. After removal of PNP the asphaltene fractions A1 and A2 are obtained in such a way that fraction A2 retains its solubility in toluene whereas fraction A1 is now insoluble in toluene and in other solvents where asphaltenes are soluble.

A plausible mechanism for the separation of these subfractions could be described as follows: In contact with PNP, molecules of subfraction A1 are displaced from the aggregate after formation of a strong hydrogen bonding complex leading to the insoluble complex PNP-A1. Removal of the phenol leads to an A1 subfraction with a solubility in toluene of

https://doi.org/10.1021/acsomega.2c06362
ACS Omega 2023, 8, 4453−4471

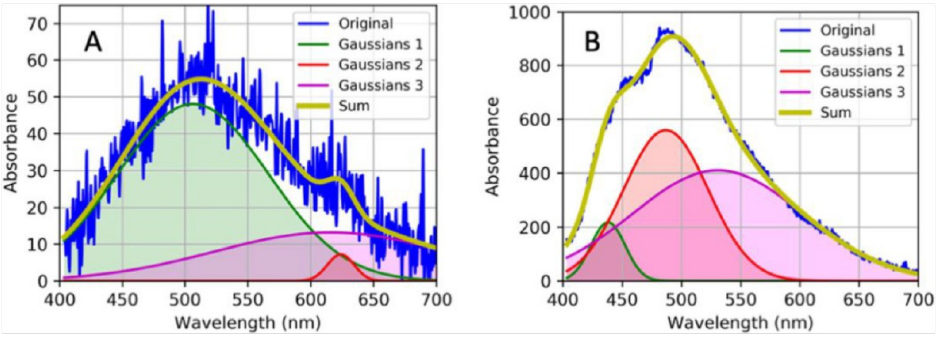

Figure 19. Fluorescence spectra for solutions before (A) and after (B) adsorption with Gaussian decomposition. Figure reprinted with permission from reference 68. Copyright 2022 Taylor and Francis.

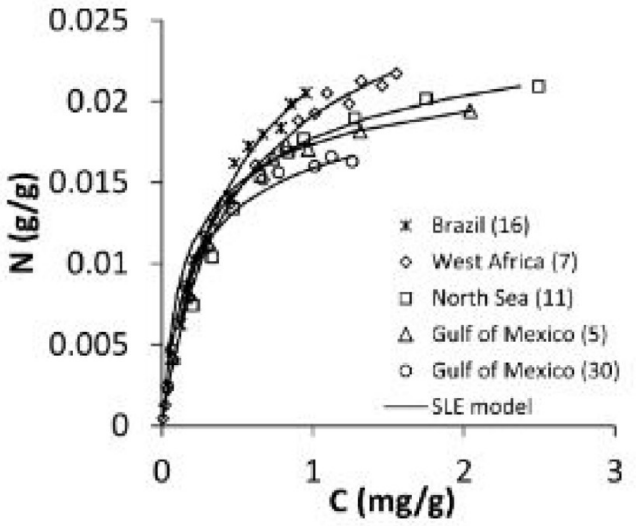

Figure 20. Isotherm adsorption of different types of asphaltenes onto $CaCO_3$. The symbols represent experimental data, and the solid lines are from the SLE model. Figure reproduced from ref 63. Copyright 2014 American Chemical Society.

barely 50 mg L^{-1}. A2-PNP and phenol excess are recovered after the usual workup;[22] see Figure 7.

In Figure 8 the pair of models used for A1 and A2 subfractions is depicted. Selection of these is largely arbitrary and based on molecular weight, and elemental analysis (C, H, N, O, and S). On the basis of differences in H/C we account for differences in aliphatic rings or DBE. Placement of functional groups of nitrogen and oxygen was arbitrary and based on the expected capacity of asphaltenes for forming aggregates. Aromatic cores were the same for these models and placement of N and OH was done on the expected formation of the hydrogen bonding's (acid−base) interaction.

Trapped Compounds. Trapped or occluded compounds are those which remain within the asphaltene aggregate and are not asphaltenes. These compounds are soluble in *n*-heptane.[23,24] We use the same PNP method to collect these compounds[23] and they have proven to be useful in geochemical and structurally studies. For instance, Creux et al.[25] found that from all 16 asphaltenes they analyzed, a series of *n*-alkaloid acid ethyl esters were found from the fraction called occluded compounds, which were generally dominated by the even-carbon-numbered *n*-alkanoic acids in the esters. The above-reported compounds inside asphaltene aggregates are interpreted as hydrocarbon representatives of materials generated from kerogen at an early stage.

Silva et al.[26] reported that the structural features of asphaltenes enable them to occlude other molecules such as biomarkers. These properties of the aggregates could hinder the secondary alteration of biomarkers that occurs in oil reservoirs; these biomarkers could, therefore, could be considered the remnants of the "original oil". For example, in this report asphaltenes from Brazilian crude oils were obtained and submitted to oxidative treatment to disrupt their structure, releasing the trapped oil. The released hydrocarbons after the treatment were compared with those from the original crude oil, and used to evaluate the alteration of the oils, especially as a result of biodegradation. The authors suggest that occluded saturated hydrocarbons represent the original oil derived from kerogen, retained and protected against alteration inside asphaltenes over geological times.[26]

Ganeeva and co-workers[26] wrote that asphaltene aggregates are made of a mixture of two fractions, the first a well-packed and stable in benzene (toluene) solution core and the second a loose-packed periphery, which can respectively occlude and adsorb other oil fractions. It was proposed by other authors[25] that the "occluded compounds have been well-protected from the secondary alteration processes that occurred in the oil reservoir and could be considered to be the original oil, whereas the adsorbed compounds have been affected by the secondary evolving processes". In this paper,[26] the compounds, adsorbed and occluded in asphaltenes both, of the crude oils of the multipay Bavly oil field (Russia) and bitumen extracted from the source bed (Domanic formation) of the same oil field are studied and compared. In this work it was found that the content of adsorbed compounds can reach up to 20% and higher and the composition is dominated by resin components (mostly the polar resins).

Marzie et al.[27] use the electron paramagnetic resonance (EPR) technique to study the behavior of the asphaltenes from the Merey crude oil (ASCM), its vacuum residue (ARVM), its fractions, and trapped compounds (A1-ASCM, A2-ASCM, TC-ASCM, A1-ARVM, A2- ARVM, and TC-ARVM). Asphaltenes were precipitated from Merey heavy crude oil and its vacuum residue. The posterior fractionation of the asphaltenes was carried out using the para-nitrophenol (PNP) method. Two fractions named A1 and A2 and trapped compounds were obtained. The temperature dependence of the EPR spectra was used to obtain a set of temperatures related to free radical (FR) generation and recombination. From the analysis of the EPR spectrum of the most intense signal of the vanadium, the temperature ranges of the anisotropic-to-isotropic domains were

https://doi.org/10.1021/acsomega.2c06362
ACS Omega 2023, 8, 4453−4471

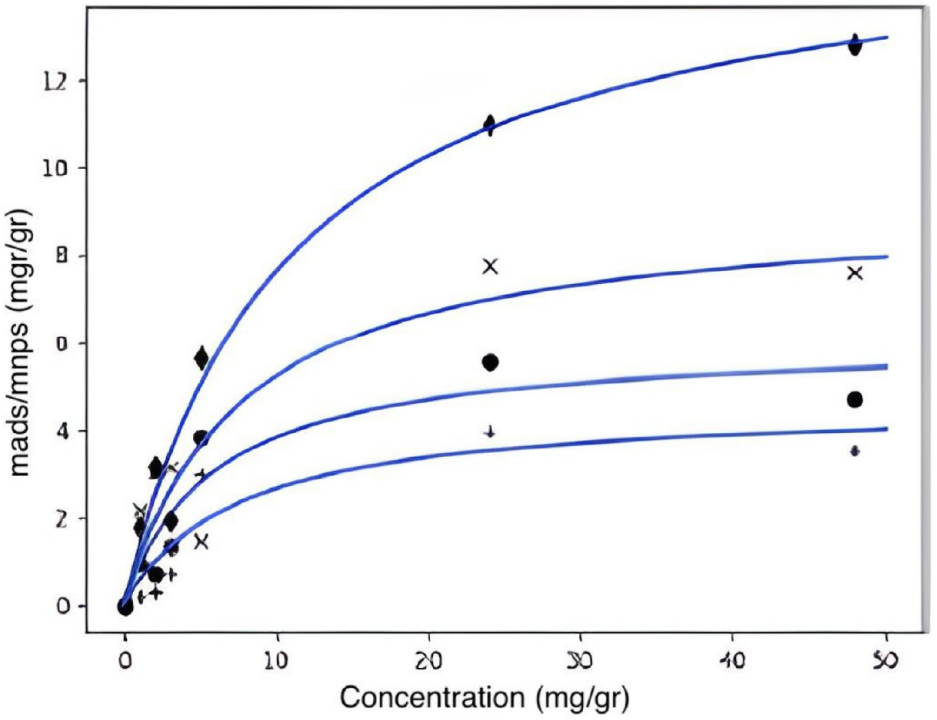

Figure 21. Adsorption plot for nanoparticles with different surface modifications. Symbols: (+) raw nanoparticles, (●) polyethylene glycol , (×) chitosan, (◆) carboximethyl cellulose (CMC).

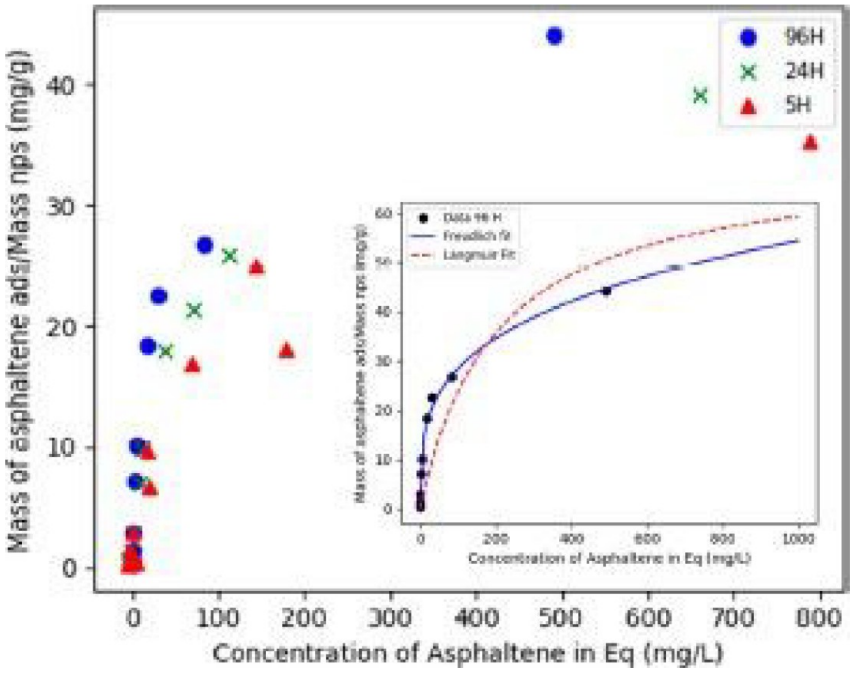

Figure 22. Adsorption plot at different times of contact and the best fitting model. Figure reproduced from ref 61. Copyright 2020 American Chemical Society.

found, and nonlinear behavior of the B parameter in the temperature range was studied. The paper reports a proposed functional relationship for parameter B as a function of the temperature. On the other hand, we found the temperatures for the slow-to-fast motion regime in these samples and correlated it with the mobility of the fractions.[28]

As reported in the work of Gray et al., the trapping of PAHs outside of the nanoaggregates during precipitation gave 7−14 times less of the quantity of PAHs in the solid precipitate. This study shows that asphaltene aggregates can interact significantly with PAHs and be included in their structure. The results are consistent with the presence of open porous asphaltene nanoaggregates in solutions, such as toluene.[27]

It was reported by Vargas et al.[29] that metal compounds such as vanadyl and nickel porphyrins present in crude oils are associated with the asphaltenes. In their work we find a

https://doi.org/10.1021/acsomega.2c06362
ACS Omega 2023, 8, 4453−4471

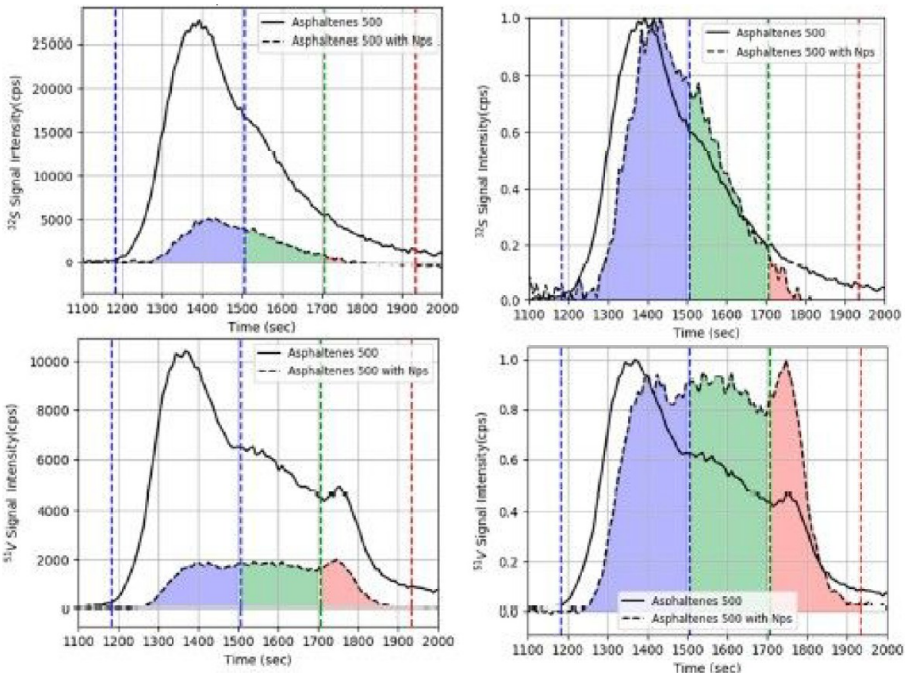

Figure 23. GPC-ICPHRMS plot showing the molecular size distribution before and after asphaltene adsorption. Figure reproduced from ref 61. Copyright 2020 American Chemical Society.

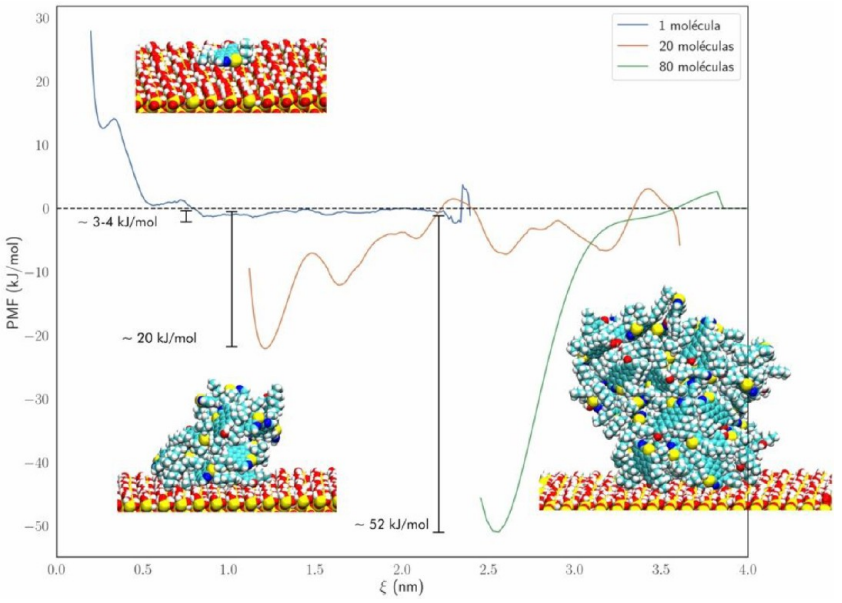

Figure 24. Theoretical calculation of different aggregates with surface (unpublished work).

dependence of the quantity on origin, maturity, pressure, and temperature. The findings suggest that during the asphaltene colloid formation the metal porphyrins could be trapped, occluded, or adsorbed, protected from aging, oxidation, or chemical degradation. In this work the authors induce the aggregation of asphaltenes by variations in the solubility parameter of the media in the presence of metal porphyrins. The UV−vis absorbance technique was use to monitored asphaltene aggregation at 350 and 405 nm to follow the porphyrin Soret band. The results showed that more than 50% of the porphyrins were trapped inside the asphaltene aggregate and posterior redissolution of the aggregates in toluene showed very low release of the porphyrins, demonstrating the strong interaction between the metallic porphyrin and asphaltenes during the aggregation.[29]

In relation to the geochemical importance of trapped compounds it has been claimed that[30]

- Asphaltenes incorporate chemical structures (trapped compounds) useful for biomarker correlation.
- Asphaltenes act as host occluding hydrocarbons that represent the original source character
- From the experiments asphaltene moieties and occlusions may be obtained independently and unambiguously.
- Analytical approaches include oxidation, reduction, and pyrolysis.

https://doi.org/10.1021/acsomega.2c06362
ACS Omega 2023, 8, 4453−4471

- Well known analytical methods may constrain the elucidation of asphaltene properties.

A report[31] of Jing et al. conclude that asphaltenes are polar macromolecules with complex structures in oils, usually forming aggregates. The findings in this work point to inside the macromolecular structures of asphaltenes, some other fractions can be adsorbed/occluded, and the occluded compounds contain important geochemical information. However, the adsorption/occlusion phenomena of asphaltenes need verification. Thus, in this work[31] the results aimed to experimentally study the adsorption/occlusion processes inside the asphaltenes, using the deuterated paraffin n-$C_{20}D_{42}$ as the target compound under the conditions of high temperature/high pressure, with some chloride salts as additives to probe the mechanism of the adsorption/occlusion inside asphaltenes.

In this contribution, Chac′on-Patiño et al.[32] use high-resolution mass spectrometry to, as they said, "unveil" the molecular composition of occluded compounds inside Colombian asphaltenes macrostructures. They focus their efforts on the fraction enriched with compounds interacting with asphaltenes via strong intermolecular forces. The experiments used normal phase column chromatography to fractionate it and atmospheric pressure photo=ionization coupled to Fourier transform ion cyclotron resonance mass spectrometry as de- tector to obtain a detailed molecular description. Their results indicate that the occluded compounds obtained in the last stage of the washing process are by themselves a complex mixture, consisting mostly of saturated compounds including molecular formulas correspond- ing to biomarkers, alkyl aromatics with high heteroatom content (up to four heteroatoms), vanadyl porphyrins, and highly aromatic species, which we believe are low-molecular weight asphaltenes transferred to the n-heptane during the extraction process.

According to Liao and co-workers,[33] within geomacromolecules, such as kerogen, asphaltene, and solid bitumen, other compounds can be adsorbed and even occluded as free molecules. According their analysis, the occluded components have been well preserved by the macromolecular structure, and retain some of the primary geochemical information. In their work they try to probe a relationship of the geochemical evolution of occluded hydrocarbons inside geomacromolecules with the geomacromolecule evolution from kerogen → asphaltene → solid bitumen. The results of their work show that occluded hydrocarbons can be transferred steadily from kerogen → asphaltene → solid bitumen. Later-evolved geomacromolecules not only inherit the occluded hydrocarbons from the former ones, but can also occlude some new free molecules. The results shown that occluded hydrocarbons are subject to a relatively independent thermal evolution, whereas the evolution of adsorbed molecules is constrained by other factors besides thermal stress. The work concludes that elucidation of the geochemical evolution of occluded hydrocarbons inside geomacromolecules will be helpful in oil (bitumen)−source correlation, identification of mixed-source reservoirs, and characterization of hydrocarbon accumulation and evolution.

Retention of alkane compounds on asphaltenes was carried out in organic solutions and studied by Lopez and co-workers.[34] In their work the distribution of retained and nonretained alkanes was assessed by GC/MS and was interpreted from the perspective of reverse phase liquid chromatography (RPLC). Their results showed that asphaltenes from unstable and stable Venezuelan crude oils behave like an alkyl-bonded phase to retain alkanes. The retention of alkanes is influenced by the structural features of the studied asphaltenes, as well as by their own structure. Asphaltenes from the unstable Furrial crude oil presented shorter but more abundant alkyl chains than asphaltenes from the stable Ayacucho crude oil and, consequently, a greater capacity to retain alkane compounds. The order of retention preference was n-alkanes, followed by cyclic isoprenoids (steranes and terpenes). Acyclic isoprenoids, including pristane and phytane were the least retained of the three alkane families. The exclusion of methylene groups, a phenomenon observed in RPLC, was also observed in asphaltenes. The authors propose this phenomenon as the responsible for the appearance of liquid-crystal-like structures in asphaltene−alkane composites and for the destabilization of asphaltene assemblies. The approach used in this work opens a new window to interpretation of the interactions of asphaltenes and alkanes at a molecular level and to understand the roles of both compound classes in the mechanisms of asphaltene precipitation and wax crystallization.

Asphaltenes and Micro-GPC ICP MS. The combine microgel permeation chromatography ion couple plasma mass spectra or GPC ICP MS technique has been used as an analytical tool in asphaltenes studies. Details of this technique have been reported earlier.[35] Before reviewing its use, it is instructive to describe the concepts involved in this case.

Figure 8 depicts the profiles usually obtained for asphaltenes in THF where it is divided in three sectors of high, medium, and low molecular mass.[35] To avoid possible confusion it is useful to remember that the experimental parameter in this case is the hydrodynamics ratio and is not the molecular mass. Here we use the terms transport and detachment in connection with these three sectors. After injection of the solution in the column, the solute within the aggregate, which could be metallic porphyrins (MP) or any other trapped compound (TC), is transported from the beginning to the band maximum without any transfer of solute from the aggregate to the media. In other words the aggregate is so big that the solute MP/TC could not be detached from the aggregate or colloid during the time required in going from the beginning until the maximum. As suggested by Figure 9, and after the maximum of the band, detachment of MP/TC is promoted by the medium size aggregates. Further detachment of MP/TC increases its retention time (see Figure 9).

Figure 9 shows the SEC ICP MM chromatographic profile for asphaltene of Boscan. THF was the mobile phase. The profile could be divided in three sectors: First is the HMW from the maximum to the left corresponding to high molecular weight sector; next is the second sector or medium molecular weight, MMW, and then is a third or low molecular weight (LMW) sector.

Figure 10 GPC ICP MS profiles corresponding to an asphaltene solution in THF with THF and Dionex as the mobile and stationary phases, respectively, under room conditions; when the detector is sulfur the signal is nearly Gaussian, deformed at long times by the presence of TC and/or MP and tailing. The profile measured with a vanadium detector afforded extensive overlap with the one measured with a sulfur detector until the maximum is achieved. In this retention time lapse the aggregate acts as transport for the TC/MP sample which acts as a passenger. At this maximum solute TC/MP would be detached from the aggregates and as a consequence the corresponding retention time will be longer, and when the

https://doi.org/10.1021/acsomega.2c06362
ACS Omega 2023, 8, 4453−4471

retention time is close to 2000 s the solute moves along with the mobile phase (red curve) and there is not more fractionation.

Metallic Porphyrines, Asphaltenes, and GPC ICP MS. The above combined GPC ICP MS technique was used to analyze Sulfur, Vanadium and Niquel in four asphaltenes and their corresponding A1 (toluene insoluble), A2 (toluene soluble), and trapped compound (TC, heptane soluble) fractions.[35] For three of the asphaltene samples, the normalized μ-SEC ICP profiles for both nickel and sulfur were very similar, showing that nickel porphyrins were distributed in almost all types of asphaltene aggregates. Extensive overlapping with sulfur profiles was observed for all vanadium and nickel profiles at retention times below the maximum bands. This fact suggests that large amounts of nickel and other organometallic or metal-porphyrin-type (MP) compounds are interlocked with asphaltene molecules, forming aggregates in solution. The process of trapping compounds within geochemical macromolecules probably occurs during petroleum formation; in other words from kerogen to oil (see above). Accordingly, no covalent bonds or specific interactions appear to be required to account for the presence of MPs within asphaltene aggregates.

Figure 11 shows chromatographic SEC HR ICP MS profiles corresponding to Boscan samples. Note that the profile corresponding to trapped compounds (TC) is shifted to the high retention time sector suggesting prevalence of a relatively low hydrodynamics ratio. The profile corresponding to A2 is clearly displaced to the large hydrodynamic ratios or very low retention time sector. Comparison of A2 with asphaltenes and A1 strongly suggests the presence of three-dimensional 3D-A2 aggregates capable of adopting conformations of longer lengths.

All samples analyzed here for Boscan are shown in Figure 11, and in reference to asphaltenes the subfraction A2 profile was shifted toward the low retention time (HMW), whereas the A1 profile was equal but the section was close to 2000. These results clearly show that when being alone subfraction A2 has the longest hydrodynamics ratio. Presumable, this condition increases the contact of A2 with the mobile phase and thus increases A2 solubility. The split of the asphaltene band in A1 and A2 bands is somewhat unexpected. In this case A2 is shifted to the lower retention times sector or large hydrodynamic ratios to obtain the result shown in Figure 11 in which case the folded A2 compound should unfold after separation from asphaltenes.

Figure 12 GPC ICP MS chromatography profiles for CN (a) and Hamaca (b) asphaltenes and subfractions A1, A2, and TC, including the super-high-molecular weight (SHMW) sector. Note that in both Figures 10 and 11, A2 subfraction contains material of very low retention time suggesting that this fraction contains the largest hydrodynamic ratio.

Model aggregates, obtained using molecular dynamics, THF as solvent, and the molecular models A12, A22, A30, and A40 are shown in Figure 13 The bands in this figure simulate the bands obtained experimentally and the similarity is qualitative. However, the results regarding the size of A2 and their possible continental structure seen in Figure 12 are very important. Note that for model A40 which is a continental type, aggregates with very long hydrodynamics ratios are obtained. Moreover, the A40 and their mixture with A30 have large cavities, easing solvent penetration and increasing solubility when compared with aggregates A12, A22, and mixture A12−A22.

The effect of silver triflate (AgOTf) on the interaction between vanadium and asphaltene nanoaggregates was investigated by gel permeation chromatography inductively cou- pled plasma high-resolution mass spectrometry (GPC ICP-HR-MS) by Bouyssiere et al.[36] Their results showed that disaggregation of some vanadium compounds linked to asphaltene nanoaggregates occurred with the reaction with silver triflate. The autors suggest that Ag^+ can partially move some porphyrins from the high-molecular-weight (HMW) region to the low-molecular-weight (LMW) region. In the work, the authors inferred that the interaction between Ag^+ and the porphyrins surroundings led to a decrease in the size of the nanoaggregates (HMW region) and an increase in the "free" V porphyrin compounds (MMW and LMW regions). Additionally shown asphaltenes from a similar origin, presenting the same vanadium GPC ICP-MS profile, gave different GPC ICP-MS profiles after AgOTf addition, which could be linked to the difference in geochemistry of the samples.

Note that these AgOTf results[36] are coherent with the above trapping of compounds in general[23,24,35,37] and with the trapping of porphyrins in particular.[36]

Super-high-molecular weight (SHMW) asphaltene aggregates, called asphaltene clusters,[38] have been observed for the first time using the above described gel permeation chromatography with inductively coupled plasma mass spectrometry (GPC-ICP-MS);[39] see Figure 12. Presumably these clusters are composed by nanoaggregates joined by physical interactions such as polar and dispersion forces forming larger aggregates. These clusters were observed for three asphaltene samples (Hamaca, Cerro Negro, and Boscan) and in their corresponding subfractions, A1 (insoluble in toluene) and A2 (soluble in toluene). Under the high dilution conditions, the experiments showed no significant change of these profiles suggesting that these clusters, as well as the other lower molecular weight (LMW) aggregates and molecules are not in chemical equilibrium with each other and behave as independent units. These results are consistent by the presence of trapped compounds within asphaltenes (TC) which are released after the *p*-nitrophenol treatment

The results corresponding to sample (b) in Figure 12 suggest the presence of large quantities of aggregates with very long hydrodynamics radius. This is coherent with results depicted in Figure 13 above which were calculated using the molecular dynamics GROMAC program (see Methods section in reference 20). According to these results and comments, the very long hydrodynamics radius, certified by the significant presence of SHMW components, as well as the porous structure of A2 (here represented by the Ao structure in Figure 12) supports the higher solubility of A2 or the archipelago-type structure.

Characterization of petroporphyrins present in the crude oil was performed by Acevedo et al. by laser ablation inductively coupled plasma mass spectrometry (LA-ICP-MS) and matrix-assisted laser desorption ionization Fourier transform ion cyclotron resonance mass spectrometry (MALDI FT-ICR MS).[40] The results presented in this paper demonstrate that even with multiple separation steps, a large quantity of vanadyl porphyrins remains inaccessible for molecular analysis by MALDI FT-ICR MS, which raises the question of what portion of a complex sample of asphaltene can be revealed by ultrahigh resolution mass spectrometry. Furthermore, the results show that easily accessible porphyrins migrate with the solvent front in HPTLC. Thus, HPTLC can be used to isolate and identify "free" porphyrins not associated with asphaltene aggregates; however, further development of separation methods is required to access the most difficult and problematic asphaltene fractions, which do

https://doi.org/10.1021/acsomega.2c06362
ACS Omega 2023, 8, 4453−4471

not migrate and impose analytical challenges due to their stronger aggregation tendency.[38]

Multiscale characterization of asphaltenes and their extrography fractions titrated with *n*-heptane was performed.[40] Chemical characterization via FT-ICR MS and GPC ICP HR-MS, stability monitoring via QCR, and AFM images of deposits indicate that "island"-enriched samples tend to form fewer, well-organized deposit aggregates, whereas samples with abundant "archipelago"-like molecules produce larger aggregates and less well-organized deposits. The combination of QCR and AFM leads to the conclusion that "island"-enriched samples lead to smaller deposits compared to "archipelago"-like molecules.

Figures 10 and 11 above suggest that when the A2 subfraction is within the asphaltene aggregates, A2 is somewhat constrained and cannot achieve the longest hydrodynamics ratio. These could be available when this fraction is detached from asphaltene in solution. These comments are coherent with an archipelago or multicore structure for A2.[40]

Distributions shown in Figure 14 are qualitatively similar to the experimental GPC-ICP- HR-MS profiles. Note that values close to 7 nm, measured in THF were also very close to other measurements in crude oil with other techniques such as SAXS[41] and TEM combined with freeze fracture where average diameters were about 10 nm.[40]

Asphaltene Adsorption. The adsorption of asphaltenes on surfaces has been extensively studied from the experimental point of view.[41−47] Adams[48] gives a fairly complete review of the results of adsorption of asphaltenes on different surfaces. The results show important peculiarities that are still under study, since there is no agreement on the mechanism of adsorption of asphaltenes and its dependence on the type of surface. A relevant point in the process is that simultaneously to the adsorption, aggregation processes are occurring in solution, and it is possible that the adsorption mechanism is by the formation of multilayers or that the adsorption is directly from aggregates.[49] In the search to determine a mechanism for the adsorption of asphaltenes on different surfaces, efforts have been made to employ very novel techniques that can provide additional information about the adsorption process.[44,50−55]

Goncalves et al.[56] use absorption and fluorescence techniques to study the aggregation process in asphaltenes solutions at relative low concentration regimes. The changes in the extinction coefficient and peak shift in the fluorescence spectra with concentration for the different samples, demonstrate the beginning of aggregation of asphaltene at concentrations as low as 50 mg/L. In Figure 15 the absorption and fluorescence intensity as a function of concentration for asphaltenes and asphaltene octylates were presented showing the aggregation at concentrations as low as 50 mg/L. This result confirms that even a low concentration of the aggregation in solution should be considered when the adsorption is studied.

Figure 16 shows an image of the surface coated with asphaltenes taken by white light interferometry. The blue stripes are the clean surface and those on the sides are the adsorbed asphaltenes. On the right are the thickness curves of the curve as a function of concentration; the thickness is directly related to the mass. As can be seen in both cases the adsorption curve presents a stepwise coating, typical of multilayer formation, but the layer thickness values indicate that the adsorbed layers are of large aggregates. A clear difference was observed for A1 and A2 aggregates, the latter having more capacity to compact and settle on the surface.

The nature of adsorbent has a critical impact in the asphaltene adsorption.[58] Comparing a raw Fe surface with an Fe nanoparticle, the differences in interaction forces were studied using atomic force microscopy. The interaction forces of asphaltenes adsorbed onto macrosurfaces with an AFM tip is 8 times higher than the interaction forces between an AFM tip and asphaltenes adsorbed onto Fe nanoparticles. This difference on the behavior of macro- and nano-surfaces could be explained on the basis of change in size and the spherical geometry of the surface inducing a reordering in the interaction forces. This results in a direct effect in the reduction of interaction between asphaltene surfaces caused by the cancellation of the induced dipole moments of the adsorbed molecules. The result of the difference in the adsorption process is reflected directly in the thickness of asphaltene adsorbed. In the case of nanoparticles few layers can be adsorbed; in the case of macro surfaces hundreds of layers can be expected.

The results in Figure 17 show the variation of the nanoparticle properties due to the asphaltene adsorption (right image). At the left, the nanoparticle size after adsorption as a function of the asphaltene concentration in the equilibrium is shown. The plot shows a saturation at low concentration and, more noticeable, a minimum coverture of 3 nm, consistent with adsorption of aggregates rather than adsorption of layers.

Asphaltene adsorption have been subject of theoretical interpretation, different models have been used to fit the experimental results of adsorption curves, from Langmuir-type models to variations such as the Freundlich or Tempkin[53,59−63] models that introduce adsorption in porous media. Farid[64] proposes a model based on a modification of the Polanyi model which is based in adsorption potential rather than physical mechanism. The Polanyi theory with the Dubinin model correlates in a good way with experimental values and is suitable for predicting adsorption phenomena. Recent studies were published by Castillo et al.[61,65] on the asphaltene interaction with SiO_2 nanoparticles produced from rice husk ash using UV−visible absorption and fluorescence spectroscopy. The adsorption vs concentration plot shows a curve well-fitted to a Dubinin−Radushkevich empirical model. This fitting function allowed the discrimination between multilayer or aggregate adsorption. Figure 18 shows the experimental points fitted with different models

The fluorescence spectra of solution before and after adsorption are presented in Figure 19. A Gaussian decomposition of the fluorescence spectra showed the preferential adsorption of a fraction associated with aggregates of high molecular weights of asphaltenes. The results presented in this work showed that the interaction between nanoparticles and asphaltenes aggregates in solution mostly occurred with larger aggregates

Cortes et al.[63] developed a solid−liquid equilibrium (SLE) model based on the "chemical theory", in their work. They claim this model accurately described the experimental data regarding different asphaltenes adsorption onto different solid surfaces (porous and nonporous) at different temperatures. In addition, according their study they found that the experimental data obtained for asphaltene adsorption fit very well to the SLE model with RSM% values lower than 10. The model was validated by several authors using different solvents, types of asphaltenes, and solid surfaces, which supposedly change the formation of molecular aggregates, irregular packing, and multilayer coverage. In Figure 20, the main results are presented for different crude oils.

https://doi.org/10.1021/acsomega.2c06362
ACS Omega 2023, 8, 4453−4471

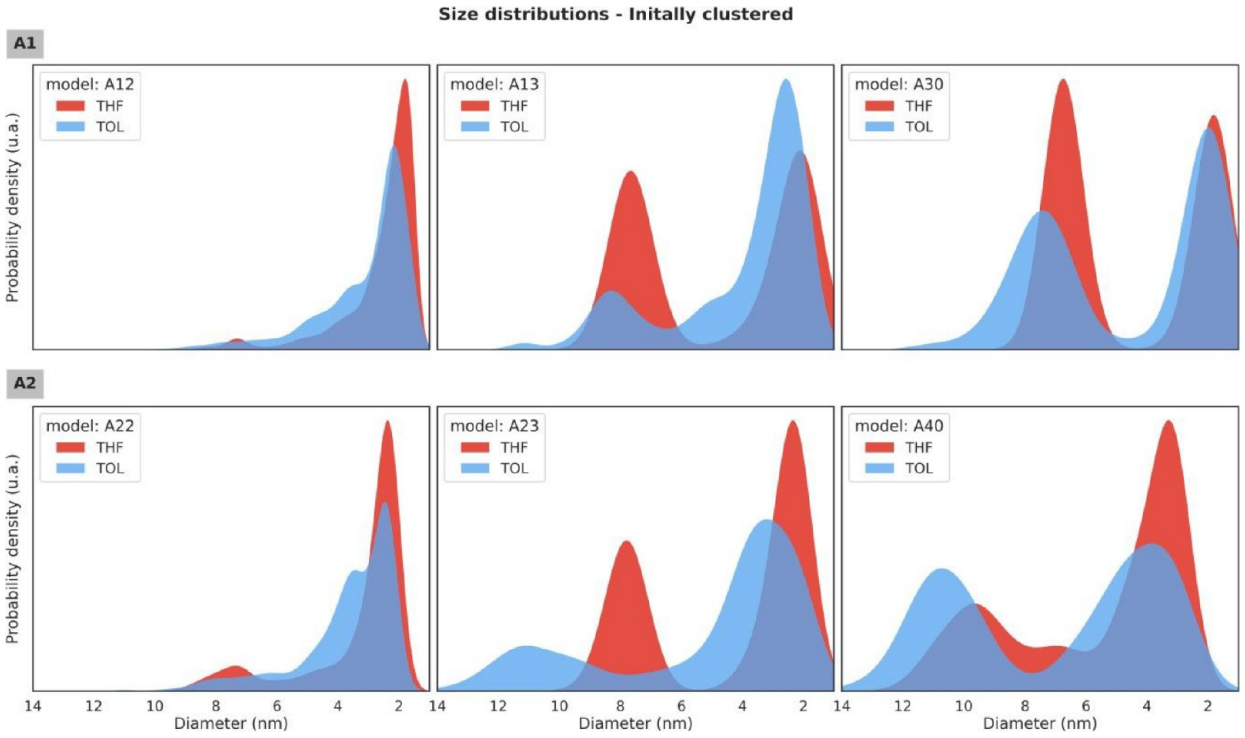

Figure 25. Histograms of the diameter of the aggregates for molecules including protic groups series labeled A1 (A12, A13, A30) and series labeled A2 (A22, A23 and A40) starting from a clustered configuration. Aggregate size increases from right to left for further comparison with GPC experiments. See Figure 1 and Table 1 for structure definition. Figure reproduced from ref 67.

Asphaltene adsorption onto raw and surface-modified SiO_2 NPs was studied by Vargas et al.[66] The results of their experiments showed an enhancement in the adsorptive properties of the NPs after the surface modification with organic compounds. The magnitude of the enhancement strongly depends on the molecular properties of the capping molecules; e.g., a 10-fold enhancement was achieved with CMC. The results in the paper show that an increment in the number of active groups in capping molecules can enhance the absorptivity of NPs. The results point to the NPs preferentially adsorbing aggregates of asphaltenes, reducing their tendency to coagulate in solution. Their result shows the possibility to increase the adsorptive capacities of NPs by modifying their surfaces with adequate molecules (Figure 21).

In recent experiments Castillo et al. employed the GPC-ICP HR MS technique to develop a methodology for analyzing changes in asphaltene in a solution in equilibrium during the adsorption onto nanoparticles.[61] In this work, variations in the CPG-ICP HR MS elution profiles of S and V and Ni were studied in samples of asphaltene in toluene before and after adsorption onto nanoparticles (Figure 22). The results presented in this paper with Ni are similar to those obtained for V, except that the sensitivity of the detector used has lower sensitivity for Ni and the signals are usually noisier. The profiles showed important changes in the proportions of the different subfractions of A1 and A2 with different molecular weights in equilibrium in asphaltene solutions (Figure 23). For all of the asphaltenes solutions analyzed, the main conclusion of the work is a different and preferential adsorption of asphaltene aggregates with a high molecular weight onto nanoparticles. The authors claim that using their developed method, a detailed information on the fractions of molecules adsorbed on nanoparticles were obtained for the first time. The observation of this preferential adsorption behavior leads to better comprehension of the adsorption onto nanoparticles and allows a plan for better methods for the mitigation of the asphaltene adsorption problem. On the basis of these results, nanoparticles have a propensity to adsorb large aggregates, and this observation contributes to develop methodologies for minimizing the aggregation and formation of new aggregates.

Theoretical calculations support the fact that large aggregates have a greater tendency to adsorb on the surface than small molecules. The sum of the hydrogen-bridge-type interactions of the aggregate surface interacts in a greater and more efficient way with the surface than small molecules or aggregates with little surface area interaction. Figure 24 presents a simulation of the interaction of aggregates of different sizes with a surface, where it is observed by the interaction energy, since the collective forces of the aggregate generate a greater interaction with the surface.

RESULTS AND DISCUSSION

Asphaltenes, Molecular Dynamics, and Micro-GPC ICP MS. The combination of these experimental and theoretical methods opens doors to study both asphaltene and asphaltene aggregates at molecular and colloidal geometric scales. To begin with, closeness between the radii measured[2] and calculated affords support to the molecular dynamic's method used here to estimate geometric factors in the aggregate or colloidal bodies. For instance, low retention times observed for A2 suggest that molecular packing in this case in looser than the one for A1 (see Figures 10 and 12). In particular for model A40, a continental-type model, very long hydrodynamic ratios (longer than 10 nm) were calculated. This was not the case for the highly aromatic, one core, island model A30. (Figures 13 and 25).

Also, a high impact on aggregation was calculated when protic hydrogen, either −OH or −COOH was included. Note that no

https://doi.org/10.1021/acsomega.2c06362
ACS Omega 2023, 8, 4453−4471

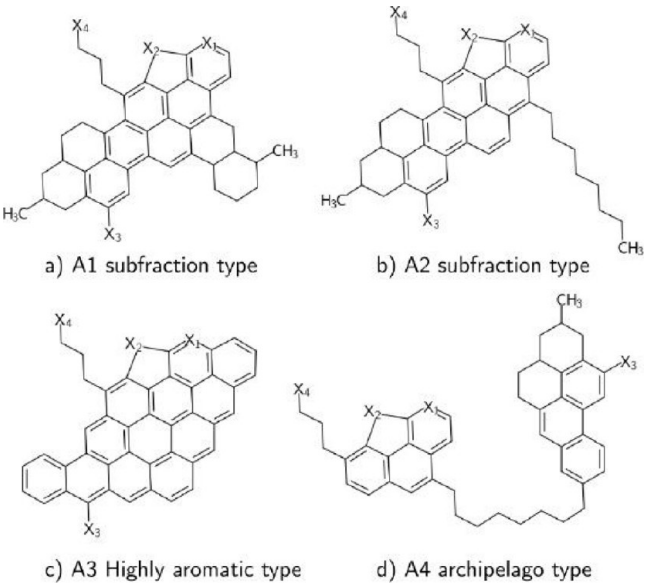

Figure 26. Molecular structure of the asphaltenes molecules used in this study for the subfractions A1 (a) and A2 (b). In addition, the A3 (c) and A4 (d) molecules are presented. X1 = N; X2 = S; X3 = −OH; X4 = Me or −COOH.

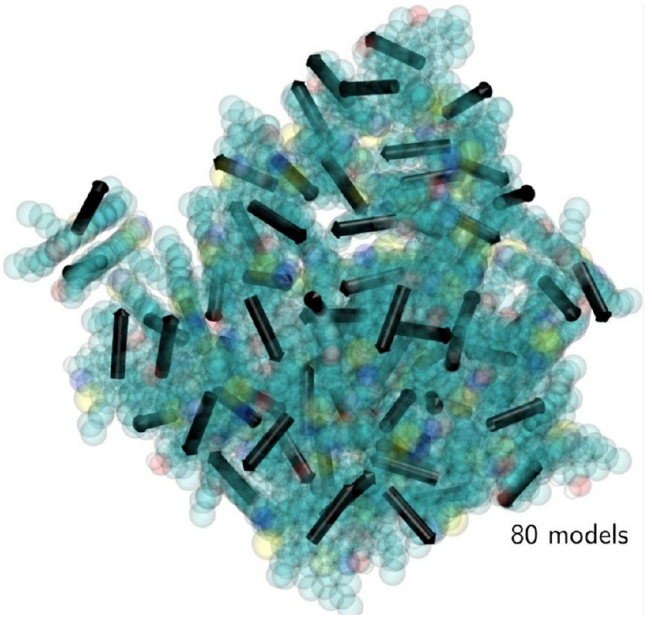

Figure 27. Illustration of dipole moments calculated by means of molecular dynamics. This corresponds to a cluster of 80 molecules in THF at room temperature. Arrows indicate dipole moment direction which in this case is equal to zero. The molecular model in this aggregate is A12.

clear trend was calculated when the solvent (toluene, THF) was changed.[43]

Molecular Dynamics and Dipole Moments. Cancellation of dipole moments (Figures 27 and 28) is a somewhat unexpected and interesting result. Apparently as the molecules in the colloid increase intermolecular forces become weaker and comparable to to that at RT.

Figure 29, taken from the literature shows several features relevant to adsorption in general and to the present work in particular. First, stepwise adsorption is depicted clearly as well as

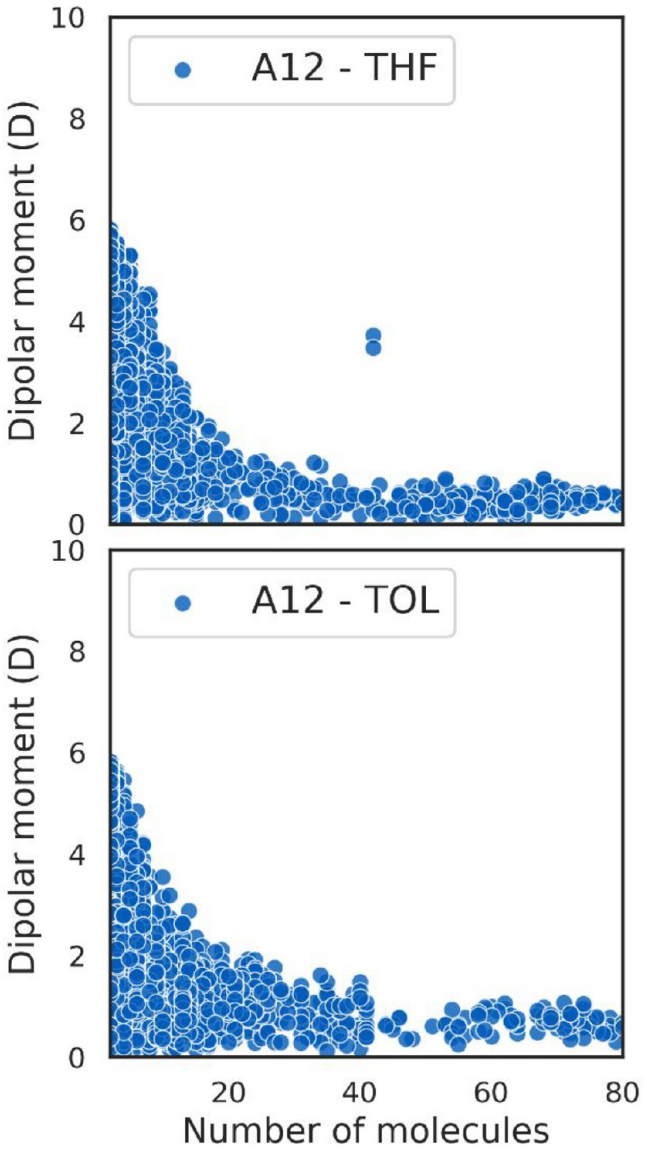

Figure 28. Reduction of the dipole moment with the increase of the number of molecules in the aggregate according to the simulation. Here we observe similar results for models A12 and A22 in toluene and THF. See also Figure 1 and Table1. Figure reproduced with permission from ref 69. Copyright 2023 Elsevier.

the time dependence of such adsorption. A glass surface is mild enough so that curved isotherms are not destroyed by the mineral adsorbent. With photothermal surface deformation (PSD) the surface could be analyzed directly allowing for accurate adsorption measurements. For convenience we choose to study the Hamaca sample. Other studied samples afforded similar results. As shown when the solution concentration is the variable, and is high enough, sudden aggregate formation in solution is followed by slow transfer of aggregates from solution to the mineral surface.

In short, for solution concentration high enough aggregate formation is collectively formed followed by a very slow aggregate adsorption. These operations are shown in Figure 30

It should be noted that events occurring in solution, such as the fast collective or sudden aggregate formation, are "recorded" by the slow transference of aggregates from the solution to the surface.

https://doi.org/10.1021/acsomega.2c06362
ACS Omega 2023, 8, 4453−4471

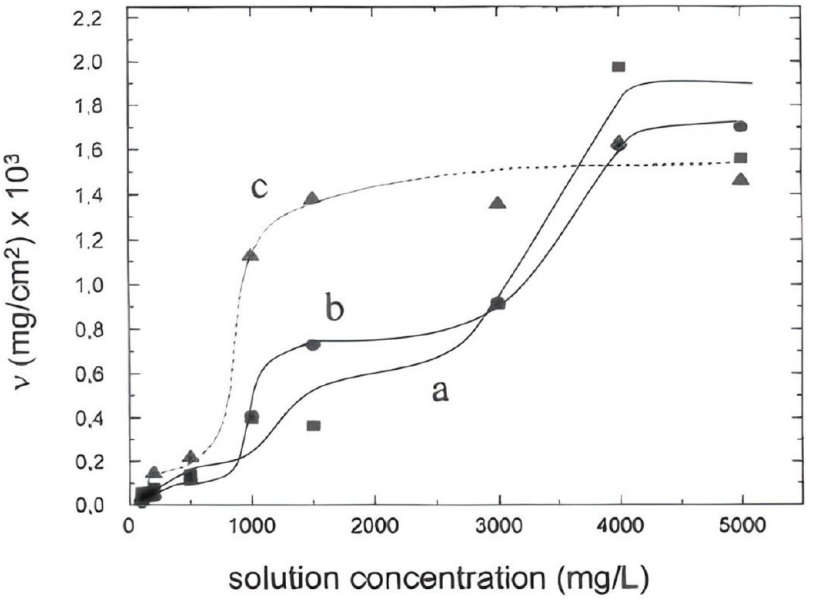

Figure 29. Adsorption isotherms for Hamaca asphaltenes onto silica plates at different times: (a) 6H, (b) 31H, and (c) 86 H.

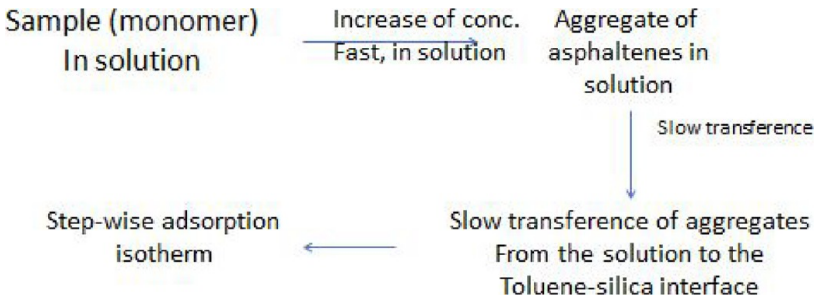

Figure 30. Diagram representing the changes required to obtain a stepwise isotherm.

Structures of the molecules involved in the simulation are shown in Figure 24. Note that aggregate structure is not dissociated by the conditions used which is coherent with the above experimental results where aggregates in solution are transferred to the interface.

AUTHOR INFORMATION

Corresponding Author

Socrates Acevedo − *Facultad de Ciencias, Escuela de Química, Universidad Central de Venezuela, Caracas 1041, Venezuela;* orcid.org/0000-0002-3069-5355; Email: socrates.acevedo@gmail.com

Author

Jimmy Castillo − *Facultad de Ciencias, Escuela de Química, Universidad Central de Venezuela, Caracas 1041, Venezuela;* orcid.org/0000-0002-6038-1074

Complete contact information is available at: https://pubs.acs.org/10.1021/acsomega.2c06362

Notes

The authors declare no competing financial interest.

ACKNOWLEDGMENTS

The authors thank the Universidad Central de Venezuela for support.

REFERENCES

(1) McLean, J. D.; Kilpatrick, P. K. Effects of Asphaltene Aggregation in Model Heptane− Toluene Mixtures on Stability of Water-in-Oil Emulsions. *J.Collo., Int. Science.* **1997**, *196*, 23−34.

(2) Groenzin, H.; Mullins, O. C. Molecular Size and Structure of Asphaltenes from Various Sources. *Energy Fuels* **2000**, *3*, 677−684.

(3) Law, J. C.; Headen, T. F.; Jimenez-Serratos, G.; Boek, E. S.; Murgich, J.; Muller, E. A. Catalogue of Plausible Molecular Models for the Molecular Dynamics of Asphaltenes and Resins Obtained from Quantitative Molecular Representation. *Energy Fuels* **2019**, *33*, 9779−9795.

(4) Ruiz-Morales, Y.; Miranda-Olvera, A. D.; Portales-Martınez, B.ın; Domınguez, J. M. Experimental and Theoretical Approach To Determine the Average Asphaltene Structure of a Crude Oil from the Golden Lane (Faja de Oro) of Mexico. *Energy Fuels* **2020**, *34*, 7985−8006.

(5) Bava, Y. B.; Gerones, M.; Buceta, D.; de la Iglesia Rodriguez, D.; Lopez-Quintela, M. A.; Erben, M. F. Elucidation of the Average Molecular Structure of Argentinian Asphaltenes. *Energy Fuels* **2019**, *33*, 2950−2960.

(6) Liu, Y.-J.; Li, Z.-F. Structural Characterization of Asphaltenes during Residue Hydrotreatment with Light Cycle Oil as an Additive. *Journal of Chemistry* **2015**, *2012*, No. 580950.

(7) Sadeghtabaghi, Z.; Rabbani, A. R.; Hemmati-Sarapardeh, A. A review on asphaltenes charac- terization by X-ray diffraction: Fundamentals, challenges, and tips. *Journal of Molecular Structure* **2021**, *1238*, 130425.

(8) Grinko, A. A.; Golovko, A. K. Fractionation of resins and asphaltenes and investigation of their composition and structure using

https://doi.org/10.1021/acsomega.2c06362
ACS Omega 2023, 8, 4453−4471

heavy oil from the USA field as an example. *Pet. Chem.* **2011**, *51*, 192−202.
(9) Goual, L.; Sedghi, M.; Wang, X.; Zhu, Z. Asphaltene Aggregation and Impact of Alkylphenols. *Langmuir* **2014**, *19*, 5394−5403.
(10) Dutta Majumdar, R.; Bake, K. D.; Ratna, Y.; Pomerantz, A. E.; Mullins, O. C.; Gerken, M.; Hazendonk, P. Single-Core PAHs in Petroleum- and Coal-Derived Asphaltenes: Size and Distribution from Solid-State NMR Spectroscopy and Optical Absorption Measurements. *Energy Fuels* **2016**, *30*, 6892−6906.
(11) Schuler, B.; Fatayer, S.; Meyer, G.; Rogel, E.; Moir, M.; Zhang, Y.; Harper, M. R.; Pomerantz, A. E.; Bake, K. D.; Witt, M.; Pena, D.; Kushnerick, J. D.; Mullins, O. C.; Ovalles, C.; van den Berg, F. G. A.; Gross, L. Heavy Oil Based Mixtures of Different Origins and Treatments Studied by Atomic Force Microscopy. *Energy Fuels* **2017**, *31*, 6856−6861.
(12) Acevedo, S; Mendez, B; Rojas, a; Layrisse, I; Rivas, H Asphaltenes and resins from the Orinoco basin. *Fuel* **1985**, *64*, 1741−1747.
(13) Acevedo, S.; Guzman, K.; Ocanto, O. Determination of the Number Average Molecular Mass of Asphaltenes (Mn) Using Their Soluble A2 Fraction and the Vapor Pressure Osmometry (VPO) Technique. *Energy Fuels* **2010**, *24*, 1809−1812.
(14) Rogel, E. Simulation of Interactions in Asphaltene Aggregates. *Energy Fuels* **2000**, *14*, 566−574.
(15) Santos Silva, H.; Alfarra, A.; Vallverdu, G.; Begue, D.; Bouyssiere, B.; Baraille, I. Impact of H-Bonds and Porphyrins on Asphaltene Aggregation As Revealed by Molecular Dynamics Simulations. *Energy Fuels* **2018**, *32*, 11153−11164.
(16) Tan, X.; Fenniri, H.; Gray, M. R. Water Enhances the Aggregation of Model Asphaltenes in Solution via Hydrogen Bonding. *Energy Fuels* **2009**, *23*, 3687−3693.
(17) da Costa, L. M.; Stoyanov, S. R.; Gusarov, S.; Tan, X.; Gray, M. R.; Stryker, J. M.; Tykwinski, R.; de M. Carneiro, J. W.; Seidl, P. R.; Kovalenko, A. Density Functional Theory Investigation of the Contributions of π-π Stacking and Hydrogen-Bonding Interactions to the Aggregation of Model Asphaltene Compounds. *Energy Fuels* **2012**, *26*, 2727−2735.
(18) Headen, T. F.; Boek, E. S.; Jackson, G.; Totton, T. S.; Muller, E. A. Simulation of Asphaltene Aggregation through Molecular Dynamics: Insights and Limitations. *Energy Fuels* **2017**, *31*, 1108−1125.
(19) Silva, H. S.; Sodero, A. C. R.; Bouyssiere, B.; Carrier, H.; Korb, J.-P.; Alfarra, A.; Vallverdu, G.; Begue, D.; Baraille, I. Molecular Dynamics Study of Nanoaggregation in Asphaltene Mixtures: Effects of the N, O, and S Heteroatoms. *Energy Fuels* **2016**, *30*, 5656−5664.
(20) Villegas, O.; Salvato Vallverdu, G.; Bouyssiere, B.; Acevedo, S.; Castillo, J.; Baraille, I. Molecular Cartography of A1 and A2 Asphaltene Subfractions from Classical Molecular Dynamics Simulations. *Energy Fuels* **2020**, *34*, 13954−13965.
(21) Gutierrez, L. B.; Ranaudo, M. A.; Mendez, B.; Acevedo, S. Fractionation of Asphaltene by Complex Formation with p-Nitrophenol. A Method for Structural Studies and Stability of Asphaltene Colloids. *Energy Fuels* **2001**, *15*, 624−628.
(22) Mujica, V.; Nieto, P.; Puerta, L.; Acevedo, S. S. Caging of Molecules by Asphaltenes. A Model for Free Radical Preservation in Crude Oils. *Energy Fuels* **2000**, *14*, 632−639.
(23) Acevedo, S.; Cordero T., J. M.; Carrier, H.; Bouyssiere, B.; Lobinski, R. Trapping of Paraffin and Other Compounds by Asphaltenes Detected by LDI TOF MS. Role of A1 and A2 Asphaltene Fractions in This Trapping. *Energy Fuels* **2009**, *23*, 842−848.
(24) Yang, C.; Liao, Z.; Zhang, L.; Creux, P. Some Biogenic-Related Compounds Occluded inside Asphaltene Aggregates. *Energy Fuels* **2009**, *23*, 820−827.
(25) Silva, T. F.; Azevedo, D. A.; Rangel, M. D.; Fontes, R. A.; Neto, F. R. A. Effect of biodegradation on biomarkers released from asphaltenes. *Org. Geochem.* **2008**, *39*, 1249−1257.
(26) Ganeeva, Y. M.; Barskaya, E. E.; Okhotnikova, E. S.; Yusupova, T. N. Features of the Composition of Compounds Trapped in Asphaltenes of Oils and Bitumens of the Bavly Oil Field. *Energy Fuels* **2021**, *35*, 2493−2505.
(27) Derakhshesh, M.; Bergmann, A.; Gray, M. R. Occlusion of Polyaromatic Compounds in Asphaltene Precipitates Suggests Porous Nanoaggregates. *Energy Fuels* **2013**, *27*, 1748−1751.
(28) Hernandez, M. S.; Silva, P. J. Electron Paramagnetic Resonance Study of the Fractions and Trapped Compounds in Asphaltenes of Merey Heavy Crude Oils and Its Vacuum Residue. *Energy Fuels* **2020**, *34*, 5641−5651.
(29) Castillo, J.; Vargas, V. Metal porphyrin occlusion: Adsorption during asphaltene ag- gregation. *Petroleum Science and Technology* **2016**, *34*, 873−879.
(30) Snowdon, L. R.; Volkman, J. K.; Zhang, Z.; Tao, G.; Liu, P. The organic geochemistry of asphaltenes and occluded biomarkers. *Org. Geochem.* **2016**, *91*, 3−15.
(31) Zhao, J.; Liao, Z.; Chrostowska, A.; Liu, Q.; Zhang, L.; Graciaa, A.; Creux, P. Experimental Studies on the Adsorption/Occlusion Phenomena Inside the Macromolecular Structures of Asphaltenes. *Energy Fuels* **2012**, *26*, 1746−1755.
(32) Chacon-Patino, M. L.; Vesga-Martinez, S. J.; Blanco-Tirado, C.; Orrego-Ruiz, J. A.; Gomez-Escudero, A.; Combariza, M. Y. Exploring Occluded Compounds and Their Interactions with Asphaltene Networks Using High-Resolution Mass Spectrometry. *Energy Fuels* **2016**, *30*, 4550−4561.
(33) Cheng, B.; Zhao, J.; Yang, C.; Tian, Y.; Liao, Z. Geochemical Evolution of Occluded Hydrocarbons inside Geomacromolecules: A Review. *Energy Fuels* **2017**, *31*, 8823−8832.
(34) Orea, M.; Ranaudo, M. A.; Lugo, P.; Lopez, L. Retention of Alkane Compounds on Asphaltenes. Insights About the Nature of Asphaltene−Alkane Interactions. *Energy Fuels* **2016**, *30*, 8098−8113.
(35) Gonzalez, G.; Acevedo, S.; Castillo, J.; Villegas, O.; Ranaudo, M. A.; Guzman, K.; Orea, M.; Bouyssiere, B. Study of Very High Molecular Weight Cluster Presence in THF Solution of Asphaltenes and Subfractions A1 and A2, by Gel Permeation Chromatography with Inductively Coupled Plasma Mass Spectrometry. *Energy Fuels* **2020**, *34*, 12535−12544.
(36) Moulian, R.; Zheng, F.; Salvato Vallverdu, G.; Barrere-Mangote, C.; Shi, Q.; Giusti, P.; Bouyssiere, B. Understanding the Vanadium−Asphaltene Nanoaggregate Link with Silver Triflate Complexation and GPC ICP-MS Analysis. *Energy Fuels* **2020**, *34*, 13759−13766.
(37) Acevedo, S.; Guzman, K.; Labrador, H.; Carrier, H.; Bouyssiere, B.; Lobinski, R. Trapping of Metallic Porphyrins by Asphaltene Aggregates: A Size Exclusion Microchro- matography With High-Resolution Inductively Coupled Plasma Mass Spectrometric Detection Study. *Energy Fuels* **2012**, *26*, 4968−4977.
(38) Moulian, R.; Chacon-Patino, M.; Lacroix-Andrivet, O.; Mounicou, S.; Mendes Siqueira, A. L.; Afonso, C.; Rodgers, R.; Giust, P.; Bouyssiere, B.; Barrere-Mangote, C. Speciation of Metals in Asphaltenes by High-Performance Thin-Layer Chromatography and Solid−Liquid Extraction Hyphenated with Elemental and Molecular Identification. *Energy Fuels* **2020**, *34*, 12449−12456.
(39) Acevedo, N.; Moulian, R.; Chacon-Patino, M. L.; Mejia, A.; Radji, S.; Daridon, J.-L.; Barrere-Mangote, C.; Giusti, P.; Rodgers, R. P.; Piscitelli, V.; Castillo, J.; Carrier, H.; Bouyssiere, B. Understanding Asphaltene Fraction Behavior through Combined Quartz Crystal Resonator Sensor, FT-ICR MS, GPC ICP HR-MS, and AFM Characterization. Part I: Extrography Fractionations. *Energy Fuels* **2020**, *34*, 13903−13915.
(40) Acevedo, N.; Moulian, R.; Chacon-Patino, M. L.; Mejia, A.; Radji, S.; Daridon, J.-L.; Barrere-Mangote, C.; Giusti, P.; Rodgers, R. P.; Piscitelli, V.; Castillo, J.; Carrier, H.; Bouyssiere, B. Understanding Asphaltene Fraction Behavior through Combined Quartz Crystal Resonator Sensor, FT-ICR MS, GPC ICP HR-MS, and AFM Characterization. Part I: Extrography Fractionations. *Energy Fuels* **2020**, *34*, 13903−13915.
(41) Franco, C. A.; Lozano, M. M.; Acevedo, S.; Nassar, N. N.; Cortes, F. B. Effects of Resin i on Asphaltene Adsorption onto Nanoparticles: A Novel Method for Obtaining Asphaltenes/Resin Isotherms. *Energy Fuels* **2016**, *30*, 264−272.
(42) Castillo, J.; Fernandez, A. Adsorption of Asphaltenes at the Toluene - Silica Interface: A Kinetic Study. *Energy Fuels* **2003**, *17*, 2−6.

https://doi.org/10.1021/acsomega.2c06362
ACS Omega 2023, 8, 4453−4471

(43) Nassar, N. N.; Hassan, A.; Pereira-Almao, P. Metal Oxide Nanoparticles for Asphaltene Adsorption and Oxidation. *Energy Fuels* **2011**, *25*, 1017−1023.
(44) Acevedo, S.; Castillo, J.; Fernandez, A.; Goncalves, S.; Ranaudo, M. A. A study of multilayer adsorption of asphaltenes on glass surfaces by photothermal surface deformation. Relation of this adsorption to aggregate formation in solution. *Energy Fuels* **1998**, *12*, 386−390.
(45) Franco, C. A.; Nassar, N. N.; Ruiz, M. A.; Pereira-Almao, P.; Cortes, F. B. Nanoparticles for Inhibition of Asphaltenes Damage: Adsorption Study and Displacement Test on Porous Media. *Energy Fuels* **2013**, *27*, 2899−2907.
(46) Hosseinpour, N.; Khodadadi, A. A.; Bahramian, A.; Mortazavi, Y. Asphaltene adsorption onto acidic/basic metal oxide nanoparticles toward in situ upgrading of reservoir oils by nanotechnology. *Langmuir* **2013**, *29*, 14135−14146.
(47) Wang, S.; Liu, Q.; Tan, X.; Xu, C.; Gray, M. R. Study of Asphaltene Adsorption on Kaolinite by X-ray Photoelectron Spectroscopy and Time-of-Flight Secondary Ion Mass Spectroscopy. *Energy Fuels* **2013**, *27*, 2465−2473.
(48) Adams, J. J. Asphaltene Adsorption, a Literature Review. *Energy Fuels* **2014**, *28*, 2831−2856.
(49) Castillo, J; Goncalves, S; Fernandez, A; Mujica, V Applications of photothermal displacement spectroscopy to the study of asphaltenes adsorption. *Optics communications* **1998**, *145*, 69−75.
(50) Acevedo, S.; Ranaudo, M.; Castillo, J.; Caetano, M.; Fernandez, A. Use of laser techniques for the study of asphaltene aggregation and adsorption. *ACS Division of Fuel Chemistry, Preprints*, 1999. *44*, (4).
(51) Zhao, J.; Liao, Z.; Chrostowska, A.; Liu, Q.; Zhang, L.; Graciaa, A.; Creux, P. Experimental studies on the adsorption/occlusion phenomena inside the macromolecular structures of asphaltenes. *Energy Fuels* **2012**, *26*, 1746−1755.
(52) Ekholm, P.; Blomberg, E.; Claesson, P.; Auflem, I. H.; Sjoblom, J.; Kornfeldt, A. A quartz crystal microbalance study of the adsorption of asphaltenes and resins onto a hydrophilic surface. *J. Colloid Interface Sci.* **2002**, *247*, 342−350.
(53) Sepideh Kashefi; Lotfollahi, M. N.; Shahrabadi, A. Asphaltene Adsorption using Nanoparticles with Different Surface Chemistry: Equilibrium and Thermodynamics Studies. *Petroleum Chemistry* **2019**, *59*, 1201−1206.
(54) Syunyaev, R. Z.; Balabin, R. M.; Akhatov, I. S.; Safieva, J. O. Adsorption of Petroleum Asphaltenes onto Reservoir Rock Sands Studied by Near-Infrared (NIR). *Spectroscopy* **2009**, *23*, 1230−1236.
(55) Subramanian, S.; Simon, S.; Gao, B.; Sjöblom, J. Asphaltene fractionation based on adsorption onto calcium carbonate: Part 1: Characterization of sub-fractions and QCM-measurements. *Colloids and Surfaces A: Physicochemical and Engineering As- pects* **2016**, *495*, 136−148.
(56) Goncalves, S.; Castillo, J.; Fernandez, A.; Hung, J. Absorbance and fluorescence spec- troscopy on the aggregation behavior of asphaltene−toluene solutions. *Fuel* **2004**, *83*, 1823−1828.
(57) Castillo, J.; Ranaudo, M.A.; Fernandez, A.; Piscitelli, V.; Maza, M.; Navarro, A. Study of the aggregation and adsorption of asphaltene sub-fractions A1 and A2 by white light interferometry: Importance of A1 subfraction in the aggregation process. *Colloids Surf., A* **2013**, *427*, 41−46.
(58) Castillo, J.; Vargas, V.; Piscitelli, V.; Ordoñez, L.; Rojas, H. Study of asphaltene adsorption onto raw surfaces and iron nanoparticles by AFM force spectroscopy. *J. Pet. Sci. Eng.* **2017**, *151*, 248.
(59) Franco, C. A.; Montoya, T.; Nassar, N. N.; Pereira-Almao, P.; Cortes, F. B. Adsorption and Subsequent Oxidation of Colombian Asphaltenes onto Nickel and/or Palladium Oxide Supported on Fumed Silica Nanoparti- cles. *Energy Fuels* **2013**, *27*, 7336−7347.
(60) Nassar, N. N.; Montoya, T.; Franco, C. A.; Cortes, F. B.; Pereira-Almao, P. A New Model for Describing the Adsorption of Asphaltenes on Porous Media at a High Pressure and Temperature under Flow Conditions. *Energy Fuels* **2015**, *29*, 4210−4221.
(61) Castillo, J.; Vargas, V.; Gonzalez, G.; Ruiz, W.; Gascon, G.; Bouyssiere, B. Development of a Methodology Using GPC-ICP HR MS for Analysis of the Adsorption of Asphaltene Aggregates on SiO2 Nanoparticles. *Energy Fuels* **2020**, *34*, 6920−6927.
(62) Mejia, J. M.; Ruiz, M. A.; Benjumea, P.; Riffel, D. B.; Cortes, F. B. Sorption of Asphaltenes onto Nanoparticles of Nickel Oxide Supported on Nanoparticulated Silica Gel. *Energy Fuels* **2012**, *26*, 1725−1730.
(63) Montoya, T.; Coral, D.; Franco, C. A.; Nassar, N. N.; Cortes, F. B. A Novel Solid− Liquid Equilibrium Model for Describing the Adsorption of Associating Asphaltene Molecules onto Solid Surfaces Based on the "Chemical Theory. *Energy Fuels* **2014**, *28*, 4963−4975.
(64) Giraldo, J.; Nassar, N. N.; Benjumea, P.; Pereira-Almao, P.; Cortes, F. B. Modeling and prediction of asphaltene adsorption isotherms using Polanyi's modified theory. *Energy Fuels* **2013**, *27*, 2908−2914.
(65) Castillo, J.; Vargas, V.; Macero, D.; Le Beulze, A.; Ruiz, W.; Bouyssiere, B. One-step synthesis of SiO_2 αFe_2O_3 Fe_3O_4 composite nanoparticles with magnetic properties from rice husks. *Physica B: Condensed Matter* **2021**, *605*, 412799.
(66) Vargas, V.; Castillo, J.; Ocampo-Torres, R.; Lienemann, C.-P.; Bouyssiere, B. Surface modification of SiO2 nanoparticles to increase asphaltene adsorption. *Petroleum Science and Technology* **2018**, *36*, 618.
(67) Villegas, O. Molecular dynamics simulations of asphaltènes and their A1 and A2 subfractions in the presence of solvents and silica nanoparticles. Ph.D. Thesis, Universite de Pau et des pays de l'adour, 2022.
(68) Castillo, J.; Vargas, V.; Gonzalez, G.; Ruiz, W.; Bouyssiere, B. Evidence of selective asphaltene subfraction adsorption on SiO2 nanoparticles studied by UV-vis absorbance and fluorescence spectroscopy. *J. Dispers. Sci. Technol.* **2022**, *43*, 873.
(69) Villegas, O.; Vallverdu, G. S.; Bouyssiere, B.; Acevedo, S.; Castillo, J.; Baraille, I. Cancellation of dipole moment of models of asphaltene aggregates as a mean for their dispersion in toluene and THF calculated using molecular dynamics. *Fuel* **2023**, *334*, 126472.

https://doi.org/10.1021/acsomega.2c06362
ACS Omega 2023, 8, 4453−4471